Roles of the cyanobacterial clock protein KaiB for the generation of circadian oscillations: importance of the monomer-dimer-tetramer interconversion of KaiB

（概日リズム発振における藍色細菌時計タンパク質 KaiB の役割：KaiB の単量体-二量体-四量体間オリゴマー構造変化の重要性）

Takahiro Iida

飯田 高広

Table of Contents

Abstract

The molecular machinery of the cyanobacterial circadian clock oscillator consists of three proteins, KaiA, KaiB, and KaiC, that interact with each other to generate circadian oscillations in the presence of ATP (the *in vitro* KaiABC clock oscillator). KaiB comprises four subunits organized as a dimer of dimers. A model that, upon interaction with KaiC, the tetrameric KaiB molecule dissociates into two molecules of dimeric KaiB was proposed (1). However, it is uncertain whether KaiB also exists as a monomer and whether the KaiB monomer can drive normal circadian oscillation. To address these questions, I constructed a new KaiB oligomer mutant with an N-terminal deletion of residues 1 to 9, $KaiB_{10–108}$. $KaiB_{10–108}$ was a monomer at 4 °C but a dimer at 35 °C. $KaiB_{10–108}$ was able to drive normal clock oscillation in an *in vitro* reconstituted KaiABC clock oscillator at 25 °C, but it was not able to drive normal circadian gene expression rhythms in cyanobacterial cells at 41 °C. Wild-type KaiB existed in equilibrium between a dimer and tetramer at lower KaiB concentrations or in the presence of 1 M NaCl. These results suggest that KaiB exists in equilibrium between a monomer, dimer, and tetramer in cyanobacterial cells.

Introduction

Circadian rhythms, oscillations in metabolic and behavioral activity with a period of about 24 h, are observed from prokaryotes to eukaryotes such as *Drosophila*, *Neurospora*, *Arabidopsis*, *Chlamydomonas*, and mammals. The rhythms (1) persists in constant conditions; (2) they are reset by external time cues such as light/dark and low/high temperature signals; and (3) their period lengths are temperature-compensated (2). A clock oscillator that generates clock oscillation is located within the cell to drive observable circadian rhythms through clock output pathways. The phase of clock oscillation is reset by light and temperature signals through clock input pathways (2, 3).

Cyanobacteria are the simplest organisms that exhibit circadian rhythms (4). The gene cluster *kaiABC* that is essential for the generation of circadian rhythms has been cloned from the cyanobacterium *Synechococcus* sp. strain PCC 7942 and analyzed in the cyanobacterium (5). The *kaiABC* clock gene cluster is composed of two operons, the *kaiA* gene and the *kaiBC* operon: KaiA protein enhances *kaiBC* expression, and KaiC protein represses the expression (5). Clock-related genes included in clock output pathways, *sasA* (6), *rpaA* (7), *labA* (8), and *cikA* (9), and that included in clock input pathways, the period-extender gene *pex* (10, 11), also have been identified (Fig. 1).

The cyanobacterial circadian clock oscillator is composed of only three clock proteins, KaiA, KaiB, and KaiC, that interact with each other to generate circadian oscillations, and it can be reconstituted *in vitro* from the three Kai proteins in the presence of ATP (the *in vitro* KaiABC clock oscillator) (12) (Fig. 1). The phosphorylation level (12) and ATPase activity (13) of KaiC and

complex formation among the three Kai proteins (14, 15) oscillate with a 24-h period in the *in vitro* KaiABC clock oscillator.

KaiA is a homodimer, and its structure has been revealed by X-ray crystallography (16-18). The KaiA subunit consists of three functional domains: the N-terminal amplitude-amplifier domain that amplifies the amplitude of clock oscillation, the central period-adjuster domain that adjusts the period length of clock oscillation to about 24h, and the C-terminal clock-oscillator domain that generates clock oscillation (17). KaiA associates with KaiC *via* the proteins' C-terminal domains (19) to enhance the ATPase (13, 20) and autokinase activities (17, 21-23) of KaiC. KaiA also associates weakly with KaiB (24). KaiA is involved in the enhancement of *kaiBC* transcription (5). The KaiC subunit has a duplicated structure, with a set of ATPase motifs in each half (5). KaiC is an ATPase with very low, temperature-compensated activity (20), and a mutant lacking two phosphorylation sites does not show the temperature-compensation (20). Its N-terminal domain exhibits only ATPase activity, whereas its C-terminal domain exhibits ATPase (20), autokinase (intersubunit phosphorylation) (19), and autophosphatase activities (25-27). KaiC is a monomer ($KaiC^{1mer}$) in the absence of ATP, and it forms a hexamer ($KaiC^{6mer}$) in the presence of ATP, as revealed by cryo-microscopy (28, 29) and crystallography (30). KaiB is an unusual homotetramer comprising two asymmetric dimers, as shown by crystallography (31-33). The KaiB tetramer ($KaiB^{4mer}$) has a positively charged cleft (PC), which is flanked by two negatively charged ridges (NRs) (32). The PC may play a role in the binding of ligands because the functionally important

residues of KaiB are concentrated on the PC (32). The NRs, which are formed by KaiB's C-terminal sequence, play a role in sustaining robust bioluminescence rhythms *in vivo* (32). The KaiB crystal structure suggests that $KaiB^{4mer}$ dissociates into dimeric KaiB ($KaiB^{2mer}$) under some conditions (32) (Fig. 1). The dimer-dimer interface, which contains a KaiA-interaction site (24) around the 64th Thr residue (T64) of KaiB (32), is probably relaxed at 40 °C (24). Previously, a dimeric KaiB mutant with a C-terminal deletion from amino acid residues 95 to 108 that lacks the NRs, named $KaiB_{1–94}$ was constructed (1, 32). KaiB associates with the N-terminal domain of KaiC (34) to suppress the ATPase (13) and autokinase (33, 35) activities of KaiC only when the ATP bound to the N-terminal ATPase motifs has been hydrolyzed (34). $KaiB_{1–94}$ can drive normal circadian clock oscillation in the *in vitro* KaiABC clock oscillator (1). Two molecules of $KaiB_{1–94}$ (a dimer) associate with one molecule of $KaiC^{6mer}$, whereas one molecule of wild-type KaiB ($KaiB_{WT}$) (a tetramer) associates with one molecule of $KaiC^{6mer}$ (1). Therefore, a model that, upon interaction with $KaiC^{6mer}$, the $KaiB_{WT}{}^{4mer}$ molecule dissociates into two $KaiB_{WT}{}^{2mer}$ molecules and that the two molecules of $KaiB_{WT}{}^{2mer}$ associate with one molecule of $KaiC^{6mer}$ was proposed (1).

Although $KaiB_{1–94}$ can drive normal circadian clock oscillation in the *in vitro* KaiABC clock oscillator, it generates only greatly weakened circadian gene expression rhythms in cyanobacterial cells (1, 32). SasA is a KaiC-binding histidine kinase in the SasA-RpaA two-component regulatory system in cyanobacteria (6, 7). SasA is involved in the main clock output pathway for the transmission of time information from the KaiABC clock oscillator to the

transcription apparatus in cyanobacteria (6, 7). SasA exists mainly as a trimer ($SasA^{3mer}$) and associates with $KaiC^{6mer}$ *via* the proteins' N-terminal domains at a molecular ratio of $SasA^{3mer}$: $KaiC^{6mer}$=1:1 (36). The association enhances the autokinase activity of SasA (36). KaiB also associates with the N-terminal domain of KaiC and competitively inhibits KaiC-SasA complex formation (34), which is the first step in the SasA-mediated clock output pathway (1). A model that the defect in circadian gene expression rhythms in cyanobacterial cells expressing $KaiB_{1–94}$ on a Δ*kaiB* genetic background is caused by inhibition of normal KaiC-SasA complex formation by $KaiB_{1–94}$ has been proposed (1).

SasA interacts with RpaA, which is an OmpR-type DNA-binding response regulator (7) (Fig. 1). In the presence of KaiC and ATP *in vitro*, the phosphate group of phosphorylated SasA is transferred to RpaA (7). LabA is considered to be involved in the repression of *kaiBC* transcription mediated by RpaA (Fig. 1), mainly during subjective early night where KaiC phosphorylation level is high (8). CikA is a divergent bacteriophytochrome with characteristic histidine protein kinase motifs and a cryptic response regulator motif (9). CikA is involved in the clock output pathway for the transmission of time information from the KaiABC clock oscillator to RpaA and acts as a negative regulator of *kaiBC* expression independent of the LabA-dependent clock output pathway (37) (Fig. 1).

Pex is a dimeric DNA-binding protein, and its structure has been revealed by X-ray crystallography (39, 40). Pex is a component of the input pathway and *pex* gene is light suppressed

(38). Pex is considered to be a repressor for suppressing *kaiA* transcription (40, 41) (Fig. 1). As revealed by mutational analysis, a 5-bp *cis*-element (AGAGA) located in the upstream region of *kaiA* is essential for the Pex-mediated repression of *kaiA* transcription (41).

It is uncertain whether KaiB exists as a monomer ($KaiB^{1mer}$) and whether $KaiB^{1mer}$ is able to drive normal circadian oscillation in the *in vitro* KaiABC clock oscillator and in cyanobacterial cells. The C-terminal amino acids 95 to 108 of KaiB is critical for $KaiB^{4mer}$ formation (1). In the KaiB crystal structure, N-terminal amino acids 1 to 14 are located at the dimer-dimer interface along with C-terminal amino acids 88 to 108 from the same subunit (32). Here, using KaiB from the thermophilic cyanobacterium *Thermosynechococcus elongatus* (42), I constructed a truncated KaiB mutant with an N-terminal deletion of residues 1 to 9, $KaiB_{10–108}$. I examined the oligomeric structure of $KaiB_{10–108}$, circadian oscillation in the *in vitro* KaiABC clock oscillator driven by $KaiB_{10-108}$, and gene expression rhythms in cyanobacterial cells driven by $KaiB_{10–108}$. I showed that the oligomeric structure of $KaiB_{10–108}$ depended on temperature. $KaiB_{10–108}$ was a monomer at 4 °C and a dimer at 35 °C. I also showed that $KaiB_{10–108}$ was able to drive normal circadian oscillation in the *in vitro* KaiABC clock oscillator at 25 °C but was not able to drive normal circadian gene expression rhythms in cyanobacterial cells at 40 °C. The findings suggest that $KaiB^{1mer}$ is involved in the generation of circadian oscillation in the KaiABC clock oscillator both *in vitro* and in cyanobacterial cells. I also showed that $KaiB_{WT}$ existed in equilibrium between a dimer and a tetramer at lower KaiB concentrations, whereas it exists as a tetramer at higher KaiB concentrations

(32). These findings suggest that KaiB exists in equilibrium between a monomer, dimer, and tetramer in cyanobacterial cells.

Materials and Methods

Protein expression and purification

I produced recombinant Kai proteins derived from *T. elongatus* using *Escherichia coli* as a host, as described previously, with modifications (23). I generated a gene construct encoding a KaiB mutant with deletion of N-terminal amino acids 1 to 9 (Fig. 2A), $KaiB_{10–108}$, using PCR-mediated site-directed mutagenesis and cloned the construct into the pGEX-6P-1 vector (Merck Millipore, Darmstadt, Germany) (p*TekaiB*$_{10–108}$). I purified $KaiB_{WT}$, $KaiB_{10–108}$, $KaiB_{1–94}$ (1), SasA, KaiA, $KaiC_{WT}$, and $KaiC_{S431D/T432D}$ mutant ($KaiC_{DD}$) contains a double Glu substitution at two phosphorylation sites, S431 and T432, which is considered to mimic the completely phosphorylated form of KaiC (36) as reported previously (24). KaiC exists as a hexamer in the presence of ATP (29); here, I used $KaiC_{WT}$ hexamer ($KaiC_{WT}^{6mer}$) and $KaiC_{DD}$ hexamer ($KaiC_{DD}^{6mer}$). I expressed $KaiB_{WT}$, $KaiB_{10–108}$, $KaiB_{1–94}$, SasA, KaiA, $KaiC_{WT}$, and $KaiC_{DD}$ at monomer, monomer, monomer, trimer, dimer, hexamer, and hexamer concentrations, respectively (see below). I estimated the protein concentration with the Bradford method (43) using a Bio-Rad Protein Assay kit (Bio-Rad, Hercules, CA, USA) with bovine serum albumin as the protein standard. The proteins were used at 4 °C unless otherwise specified.

Estimation of the molecular masses of KaiB with gel filtration chromatography (GFC)

I estimated the molecular masses of $KaiB_{WT}$ and the KaiB mutants ($KaiB_{1–94}$ and $KaiB_{10–108}$) with

GFC on a Superdex 75 5/150GL column (GE Healthcare, Fairfield, CA, USA), using a Gel Filtration Calibration Kit LMW (GE Healthcare) for the molecular mass standards. Using an ÄKTA explorer (GE Healthcare), molecular masses were assessed under the following different buffer conditions: 20 mM HEPES-HCl buffer (pH 7.5) (reaction buffer), 20 mM HEPES-HCl buffer (pH 7.5) containing 300 mM NaCl, 20 mM HEPES-HCl buffer (pH 7.5) containing 500 mM NaCl, 20 mM HEPES-HCl buffer (pH 7.5) containing 1 M NaCl, 20 mM MES-NaOH buffer (pH 5.5) containing 150 mM NaCl, 20 mM MES-NaOH buffer (pH 6.5) containing 150 mM NaCl, and 20 mM Tris-HCl buffer (pH 8.5) containing 150 mM NaCl at 4 °C. KaiB was dissolved in reaction buffer unless otherwise specified. To exchange the KaiB sample buffer for another buffer (see above), the KaiB samples were subjected to GFC on a 5-mL HiTrap Desalting column (GE Healthcare) equilibrated with the exchange buffer. KaiB (4.0 μM, 12 μM, 24 μM, and 48 μM) was incubated for 6 h or 16 h at 4 °C, 15 °C, 20 °C, 25 °C, 30 °C, 35 °C, or 40 °C and then subjected to GFC at 4 °C. I monitored the elution profiles of the proteins from the absorbance at 280 nm (A_{280}). When two chromatogram peaks overlapped, I separated them numerically using PeakFit (Systat, San Jose, CA, USA).

Sedimentation equilibrium analysis (SE) of KaiB with analytical ultracentrifugation

I performed SE analysis of KaiB ($KaiB_{WT}$ and $KaiB_{10–108}$) using a Beckman Optima XL-A analytical ultracentrifuge with an An60Ti rotor. Samples were dialyzed against reaction buffer, which was used as the blank. KaiB was incubated at 4 °C or 35 °C for 16 h and then subjected to SE analyses at 4 °C

at 38,000, 40,000, and 42,000 rpm ($KaiB_{10–108}$); at 4 °C at 24,000, 26,000, and 28,000 rpm ($KaiB_{WT}$); and at 35 °C at 24,000, 26,000, and 28,000 rpm ($KaiB_{WT}$ and $KaiB_{10–108}$). I monitored the concentration profiles of the samples from the A_{280} and recorded them at a spacing of 0.001 cm in step mode, with 20 averages per step. I analyzed equilibrium data using the Beckman Optima XL-A/XL-I data analysis software, version 6.04, which was provided as an add-on to version 6.0 (Beckman Coulter, Brea, CA, USA). I calculated global, single-species fits using different KaiB concentrations (0.62 mg/ml, 0.73 mg/ml, and 0.83 mg/ml for $KaiB_{10–108}$ (4 °C); 0.53 mg/ml and 0.66 mg/ml for $KaiB_{10–108}$ (35 °C); 0.37 mg/ml, 0.48 mg/ml, and 0.56 mg/ml for $KaiB_{WT}$ (4 °C); 0.38, 0.48, and 0.58 mg/ml for $KaiB_{WT}$ (35 °C)). I calculated the partial specific volumes of the proteins from their amino acid compositions, using the partial specific volumes of amino acids described in "Analytical ultracentrifugation in biochemistry and polymer science" (44). The partial specific volumes used were 0.7487 ml/g for $KaiB_{10–108}$ (4 °C), 0.76185 ml/g for $KaiB_{10–108}$ (35 °C), 0.7497 ml/g for $KaiB_{WT}$ (4 °C), and 0.76285 ml/g for $KaiB_{WT}$ (35 °C). I used the default density value of Optima XL-A/XL-1data analysis software, version 6.04 as density of the solution in the analyses.

Measurement of the circular dichroism (CD) spectra of KaiB

I measured the CD spectra of $KaiB_{WT}$ and the KaiB mutants ($KaiB_{1–94}$ and $KaiB_{10–108}$; 40 μM each) at 4 °C in reaction buffer over a wavelength range of 200–260 nm using a spectropolarimeter equipped with a thermally jacketed quartz cuvette with a 1-mm path length (Jasco JA-720W; JASCO,

Tokyo, Japan).

Surface plasmon resonance (SPR) analyses of the interactions of KaiB with KaiC^{6mer}

I analyzed the interactions of KaiB ($KaiB_{WT}$, $KaiB_{1–94}$, $KaiB_{10–108}$) with immobilized $KaiC_{DD}{}^{6mer}$ at 25 °C with SPR using a Biacore T200 and the associated software (GE Healthcare). I immobilized 10 μM $KaiC_{DD}{}^{6mer}$ on a CM5 sensor chip using an amine coupling kit (GE Healthcare) in reaction buffer containing 0.1 mM ATP, 5 mM $MgCl_2$, 0.1 mM dithiothreitol (DTT), and 50 mM NaCl. To allow KaiB oligomeric structures to reach equilibrium, KaiB (0.5 nM, 1.0 nM, 2.0 nM, 5.0 nM, and 10 nM) was stored at 4 °C for 16 h in reaction buffer containing 1 mM ATP, 5 mM $MgCl_2$, and 0.05 % Tween 20; aliquots of the $KaiB_{10–108}$ sample were further incubated at 40 °C for 2 h ("preincubated $KaiB_{10–108}$"). The KaiB samples were stored at 15 °C ($KaiB_{WT}$, $KaiB_{1–94}$, and $KaiB_{10–108}$) or 35 °C ("preincubated $KaiB_{10–108}$") in the sample rack of a Biacore T200 until SPR measurements at 25 °C. I monitored the association and dissociation between KaiB and immobilized $KaiC_{DD}{}^{6mer}$ continuously at stepwise KaiB concentrations of 0.5 nM, 1.0 nM, 2.0 nM, 5.0 nM, and 10 nM in reaction buffer containing 1 mM ATP, 5 mM $MgCl_2$, and 0.05 % Tween 20 at 25 °C. I computed the dissociation (k_d) and association (k_a) rates by fitting a 1:1 binding model to the experimental data and calculated the value for the apparent equilibrium dissociation constant (K_D) as k_d/k_a.

Estimation of the stoichiometry of the KaiB-KaiC^{6mer} complex using GFC

Reaction mixtures containing 20 μM KaiB ($KaiB_{WT}$, $KaiB_{1–94}$, $KaiB_{10–108}$, or "preincubated $KaiB_{10–108}$") and 1 μM $KaiC_{DD}{}^{6mer}$ in reaction buffer containing 1 mM ATP and 5 mM $MgCl_2$ were incubated at 4 °C or 40 °C for 20 h and then subjected to GFC on a Superdex 200 HR 10/300 column (GE Healthcare) equilibrated with reaction buffer containing 0.1 mM ATP and 5 mM $MgCl_2$ at 4 °C. Chromatography fractions containing KaiB-KaiC^{6mer} complexes (9.4–9.6 ml for $KaiB_{10–108}$ (40 °C); 9.6–9.8 ml for $KaiB_{WT}$ (40 °C); 9.8–10.0 ml for $KaiB_{WT}$ (4 °C), $KaiB_{1–94}$ (4 °C), and $KaiB_{10–108}$ (4 °C); or 10.0–10.2 ml for $KaiB_{1–94}$ (40 °C)) were collected. Aliquots of the chromatography fractions and standard amounts of $KaiB_{WT,}$ $KaiB_{1–94}$, $KaiB_{10–108}$, and $KaiC_{DD}{}^{6mer}$ were then subjected to sodium dodecyl sulfate-polyacrylamide gel electrophoresis (SDS-PAGE) (45) on 18% gels. The gels were stained with Coomassie Brilliant Blue (CBB). I determined the amounts of KaiB and $KaiC_{DD}{}^{6mer}$ in the KaiB-KaiC^{6mer} complexes with densitometry using a CS analyzer (ATTO, Tokyo, Japan). The arginine contents of $KaiB_{WT}$, $KaiB_{1–94}$, $KaiB_{10–108}$, $KaiC_{DD}{}^{6mer}$, and BSA are 4.4%, 5.1%, 3.9%, 6.9%, and 4.3 %, respectively. The bias in the arginine contents of these proteins results in underestimation or overestimation of the protein concentration when using a Bio-Rad Protein Assay kit. These concentrations were corrected based on those determined from the bicinchoninic acid (BCA) method (46) using a BCA protein assay reagent (Thermo Fisher Scientific, Waltham, MA, USA).

Assay for the ATPase activity of KaiC

I measured the ATPase activity of $KaiC^{6mer}$ ($KaiC_{WT}{}^{6mer}$ and $KaiC_{DD}{}^{6mer}$) at 4 °C, 15 °C, 25 °C, and 40 °C using ADP-Glo Kinase Assay (Promega, Fitchburg, WI, USA) according to the supplier's instruction manual. I incubated 1 μM $KaiC^{6mer}$ in reaction buffer containing 1 mM ATP and 5 mM $MgCl_2$ at 4 °C, 15 °C, 25 °C or 40 °C for 20 h and then measured the bioluminescence signal of the samples using an ARVO X4 plate reader (PerkinElmer, Waltham, MA, USA). I calculated the amount of ADP produced from ATP and expressed the ATPase activity as mol ADP produced per mol $KaiC^{6mer}$ per h at 4 °C, 15 °C, 25 °C or 40 °C.

Assay for the *in vitro* phosphorylation rhythms of KaiC

Reaction mixtures containing 0.75 μM KaiA, 3.0 μM KaiB ($KaiB_{WT}$ or $KaiB_{10–108}$), and 0.5 μM $KaiC_{WT}{}^{6mer}$ in reaction buffer containing 1 mM ATP and 5 mM $MgCl_2$ were incubated at 25 °C. Every 4 h, 12-μl aliquots of the reaction mixtures were collected and subjected to SDS-PAGE on 12.5% gels (acrylamide:bisacrylamide = 144:1). The gels were stained with CBB. KaiC appears as triplet bands on SDS-PAGE gels; the upper two bands correspond to the phosphorylated forms of KaiC (p-KaiC), and the lowest band corresponds to the nonphosphorylated form of KaiC (np-KaiC) (19). I calculated the ratio of p-KaiC to total KaiC (the phosphorylation level of KaiC) by measuring the relative amounts of p-KaiC and np-KaiC with densitometry using a CS Analyzer (ATTO). I simulated circadian oscillations using the RAP rhythm-analyzing program (47).

In vivo bioluminescence rhythm assay

I measured the bioluminescence rhythms of *T. elongatus* strains carrying a P_{psbA1}::Xl *luxAB* reporter gene (48) at 41 °C using a high-sensitivity bioluminescence monitoring apparatus (Onai *et al*. unpublished; model CL96S-4; Churitsu Electric Co. Nagoya, Japan). I analyzed the bioluminescence rhythms with the cosinor-rhythmometry method (47, 49) using bioluminescence-analyzing software (Onai *et al*. unpublished; Kai-Seki Ninja SL00-01; Churitsu Electric Co.). The amplitude of the rhythms was calculated as the average ratios of peak to trough in each cycle.

Assay for KaiC-SasA complex formation using GFC

I measured KaiC-SasA complex formation and its inhibition by KaiB using GFC as described previously (1). Reaction mixtures containing 1.5 μM SasA and 0.75 μM $KaiC_{DD}^{6mer}$ were incubated with or without 12.0 μM KaiB ($KaiB_{WT}$, $KaiB_{1–94}$, $KaiB_{10–108}$ or "preincubated $KaiB_{10–108}$") in reaction buffer containing 1 mM ATP, 5 mM $MgCl_2$, and 0.1 mM DTT at 25 °C for 18 h. The samples were then subjected to GFC on a Superdex 200 HR 10/300 column (GE Healthcare) equilibrated with reaction buffer containing 0.1 mM ATP, 5 mM $MgCl_2$, and 0.1 mM DTT at 4 °C. Aliquots of the chromatography fractions were subjected to SDS-PAGE on 18% gels, and the gels were stained with CBB.

Results

Temperature-dependent changes in the oligomeric structure of $KaiB_{10–108}$ in solution

It was predicted that $KaiB_{10–108}$ would be a dimer because it lacks an N-terminal sequence that is located at the dimer-dimer interface of KaiB (Fig. 2A) (32). A preliminary experiment suggested that the apparent molecular mass of $KaiB_{10–108}$ depended on temperature (data not shown). Thus, I determined the oligomeric structure of $KaiB_{10–108}$ in solution at various temperatures using sedimentation equilibrium analytical ultracentrifugation and analytical gel filtration chromatography.

I estimated the molecular mass of $KaiB_{10–108}$ (subunit molecular mass, 11.4 kDa) in 20 mM HEPES-HCl buffer (pH 7.5) containing 150 mM NaCl (reaction buffer) using SE (Fig. 2B and C and Table 1). Unexpectedly, $KaiB_{10–108}$ sedimented as a 12.8 ± 0.6-kDa (n = 3) protein, corresponding to a monomer ($KaiB_{10–108}^{1mer}$) at 4 °C, whereas it sedimented as a 28 ± 0.9-kDa (n = 3) protein, corresponding to a dimer ($KaiB_{10–108}^{2mer}$) at 35 °C. Residual plots for the monomer model curve (4 °C) and dimer model curve (35 °C) fitted to the sedimentation profiles showed that higher order associations and dissociations did not occur at either 4 °C or 35 °C (Fig. 2B and C).

I also estimated the molecular mass of $KaiB_{10–108}$ at various temperatures using GFC (Fig. 2F and Table 1). When $KaiB_{10–108}$ (24 μM) was incubated at 4 °C, 15 °C, 35 °C, and 40 °C for 6 h and subjected to GFC in reaction buffer at 4 °C, it eluted as a single peak corresponding to a globular protein with molecular masses of 23.5 ± 0.0 kDa (n = 3), 23.1 ± 0.0 kDa (n = 3), 39.0 ± 0.7 kDa (n = 3), and 35.7 ± 0.0-kDa (n = 3), respectively. On the other hand, when $KaiB_{10–108}$ (24 μM) was

incubated at 20 °C, 25 °C, and 30 °C before GFC, it eluted as two peaks corresponding to a 23-kDa globular protein and a 39-kDa globular protein. The percentage of the 39-kDa protein increased at higher temperatures between 15 °C and 35 °C (Fig. 2F). The molecular mass values of $KaiB_{10–108}$ estimated at 4 °C and 40 °C using GFC were 1.8- and 1.3-times higher than those determined using SE, respectively (Table 1). The molecular mass value of $KaiB_{WT}$ estimated at 4 °C using GFC was also 1.5-times higher than that determined using SE (Table 1). In contrast, the molecular mass values of $KaiB_{1–94}$ estimated here with GFC (Table 1) were consistent with those determined with SE previously (1, 32). SE provides a reliable estimate of the molecular mass of a protein (50), while GFC provides an estimate of protein size (Stokes radius), and the molecular mass value estimated using GFC is affected by the shape and interaction of the protein with the matrix (50). Hereafter, I used the molecular mass values of $KaiB_{10\text{-}108}$, $KaiB_{WT}$, and $KaiB_{1\text{-}94}$ estimated using SE as their molecular masses. Thus, $KaiB_{10\text{-}108}{}^{1mer}$, $KaiB_{10\text{-}108}{}^{2mer}$, and $KaiB_{WT}{}^{4mer}$ eluted as a single peak corresponding to a globular protein with molecular masses of 23 kDa, 39 kDa, and 65-67 kDa, respectively, in GFC. I concluded that the oligomeric structure of $KaiB_{10–108}$ depended on temperature and that $KaiB_{10–108}$ existed in equilibrium between a monomer and dimer. Thus, I succeeded to produce a KaiB oligomeric structure mutant with an N-terminal deletion, $KaiB_{10–108}$, whose oligomeric structure as a monomer or dimer can be controlled by temperature.

For controls, I also estimated the molecular mass of $KaiB_{WT}$ (24 μM) (subunit molecular mass, 12.4 kDa) using SE and GFC and the molecular mass of $KaiB_{1–94}$ (24 μM) (subunit molecular

mass, 10.9 kDa) using GFC at various temperatures. The oligomeric structures of $KaiB_{WT}$ and $KaiB_{1–94}$ were not significantly affected by temperature, unlike that of $KaiB_{10–108}$ (Table 1). Residual plots of $KaiB_{WT}$ for the tetramer model curve fitted to the sedimentation profiles showed that higher order associations and dissociations did not occur at 4 °C or 35 °C (Fig. 2D and E). Consistent with previous observations (1, 32), these results indicate that $KaiB_{WT}$ and $KaiB_{1–94}$ existed as a tetramer ($KaiB_{WT}^{4mer}$) (32) and dimer ($KaiB_{1-94}^{2mer}$) (1), respectively, irrespective of the temperature.

Using spectropolarimetry, I confirmed that the secondary structure of $KaiB_{10–108}$ was not disrupted by the N-terminal deletion in $KaiB_{10-108}$. The CD spectrum of $KaiB_{10–108}$ was similar to the spectra of $KaiB_{WT}$ and $KaiB_{1–94}$ (Fig. 3) (32), which indicates that the secondary structure of $KaiB_{10–108}$ is similar to the structures of $KaiB_{WT}$ and $KaiB_{1–94}$.

Factors affecting KaiB oligomeric structure changes in solution

Previously, on the basis of the KaiB crystal structure, the possibility that changes in pH or ionic strength destabilize the interdimer interface of the $KaiB^{4mer}$ molecule to dissociate the molecule into the two dimers (32). The isolation of two KaiB oligomeric structure mutants, $KaiB_{1–94}$ (a dimer) and $KaiB_{10–108}$ (a monomer or dimer), suggests that KaiB can exist as a monomer, dimer, or tetramer. To identify factors other than temperature that affect the oligomeric structure of KaiB, I used GFC to examine the apparent molecular masses of $KaiB_{WT}$, $KaiB_{10–108}$, and $KaiB_{1–94}$ under various conditions, including changes in KaiB concentration, NaCl concentration, and pH.

First, I examined the effects of the KaiB concentration on the oligomeric structure of KaiB. KaiB ($KaiB_{WT}$, $KaiB_{1–94}$ or $KaiB_{10–108}$) was incubated at various concentrations for 6 h at 4 °C and then subjected to GFC at 4 °C. Samples of 12 μM, 24 μM, and 48 μM $KaiB_{WT}$ eluted as single peaks corresponding to a 64.6 ± 0.0-kDa protein (a tetramer), a 66.7 ± 1.3-kDa protein (a tetramer), and a 64.6 ± 0.0-kDa protein (a tetramer), respectively. On the other hand, 4.0 μM $KaiB_{WT}$ eluted as two peaks corresponding to a 64.6 ± 0.0-kD protein (a tetramer) and a 32.9 ± 0.6-kDa protein (a dimer) (Fig. 4A and Table 2). Thus, the oligomeric structure of $KaiB_{WT}$ as a tetramer or a dimer changed depending on the $KaiB_{WT}$ concentration. Samples of 4.0 μM, 12 μM, 24 μM, and 48 μM $KaiB_{1–94}$ eluted as single peaks corresponding to a 21.7 ± 0.4-kDa protein (a dimer), a 23.7 ± 0.0-kDa protein (a dimer), a 24.8 ± 0.0-kDa protein (a dimer), and a 25.4 ± 0.0-kDa protein (a dimer), respectively. The apparent molecular mass of $KaiB_{1–94}$ was only slightly smaller at lower $KaiB_{1–94}$ concentrations (Fig. 4B and Table 2), suggesting that the oligomeric structure of $KaiB_{1–94}$ was scarcely affected by the $KaiB_{1–94}$ concentration at the concentrations examined. $KaiB_{10–108}$ (4.0 μM, 12 μM, 24 μM, and 48 μM) eluted as a single peak corresponding to a monomer (Fig. 4C and Table 2). Thus, the oligomeric structure of $KaiB_{10–108}$ was not affected by the $KaiB_{10–108}$ concentration at the concentrations examined.

The oligomeric structure of $KaiB_{WT}$ did not depend on temperature under the conditions examined (4 °C and 40 °C), as described above (Table 1). Next, I examined the effects of temperature on the oligomeric structure of $KaiB_{WT}$ at lower $KaiB_{WT}$ concentrations, at which

$KaiB_{WT}$ existed as a mixture of $KaiB_{WT}^{2mer}$ and $KaiB_{WT}^{4mer}$. When $KaiB_{WT}$ (4.0 μM) was incubated at 40 °C for 6 h and then subjected to GFC at 4 °C, the elution profile was similar to that of $KaiB_{WT}$ incubated at 4 °C for 6 h (Fig. 4D). This result indicates that the equilibrium between $KaiB_{WT}^{4mer}$ and $KaiB_{WT}^{2mer}$ did not depend on temperature at the temperatures examined. The oligomeric structure of $KaiB_{10–108}$ did not depend on the $KaiB_{10–108}$ concentration under the conditions examined above (Table 2). Next, I examined the effects of the $KaiB_{10–108}$ concentration on the oligomeric structure of $KaiB_{10–108}$ at 25 °C, at which $KaiB_{10–108}$ existed as a mixture of $KaiB_{10–108}^{1mer}$ and $KaiB_{10–108}^{2mer}$. When $KaiB_{10–108}$ (4.0 μM and 24 μM) was incubated at 25 °C for 6 h and then subjected to GFC at 4 °C, less $KaiB_{10–108}^{2mer}$ appeared in the elution profile of 4.0 μM $KaiB_{10–108}$ than in that of 24 μM $KaiB_{10–108}$ (Fig. 4E), indicating that the equilibrium between $KaiB_{10–108}^{1mer}$ and $KaiB_{10–108}^{2mer}$ depended on the $KaiB_{10–108}$ concentration.

I then examined the effects of the NaCl concentration on the oligomeric structure of $KaiB_{WT}$. $KaiB_{WT}$ (24 μM) was incubated in 20 mM HEPES-HCl buffer (pH 7.5) containing 150 mM, 300 mM, 500 mM or 1 M NaCl at 4 °C for 16 h and then subjected to GFC at 4 °C. The peak position of $KaiB_{WT}$ in the presence of 150 mM, 300 mM, and 500 mM NaCl corresponded to a 66.7 ± 1.3-kDa protein, a 66.1 ± 1.3-kDa protein, and a 63.8 ± 1.3-kDa protein, respectively, indicating that the NaCl concentration had little, if any, effect on the oligomeric structure of $KaiB_{WT}$ within the NaCl concentration range tested. On the other hand, in the presence of 1 M NaCl, $KaiB_{WT}$ eluted as two peaks corresponding to a 63.6 ± 0.0-kD a protein (a tetramer) and a 36.8 ± 0.0-kDa protein (a dimer)

(Fig. 4F and Table 3). Thus, the oligomeric structure of $KaiB_{WT}$ as a tetramer or a dimer changed depending on the NaCl concentration. $KaiB_{WT}{}^{4mer}$ dissociated into $KaiB_{WT}{}^{2mer}$ in a high concentration of NaCl.

Next, I examined the effects of pH (buffer) on the oligomeric structure of $KaiB_{WT}$ in the presence of 150 mM NaCl. $KaiB_{WT}$ (24 μM) was incubated at 4 °C for 16 h in 20 mM MES-NaOH buffer (pH 5.5), 20 mM MES-NaOH buffer (pH 6.5), 20 mM HEPES-NaOH buffer (pH 7.5) or 20 mM Tris-HCl buffer (pH 8.5), all containing 150 mM NaCl, and subjected to GFC at 4 °C. The oligomeric structure of $KaiB_{WT}$ was not significantly affected by pH in the range examined here (Table 3).

Interaction of $KaiB_{10–108}$ with KaiC

Previously, It has been demonstrated using SPR analysis that the $KaiB_{1–94}$-$KaiC_{DD}$ association was 14.6 times stronger than the $KaiB_{WT}$-$KaiC_{DD}$ association (1). Here, I analyzed the interaction of $KaiB_{10–108}$ with $KaiC_{DD}{}^{6mer}$ at 25 °C using SPR analysis. For the interaction with $KaiC_{DD}{}^{6mer}$, the K_A (=1/K_D) value of $KaiB_{10–108}$ (0.5 nM, 1.0 nM, 2.0 nM, 5.0 nM, and 10 nM) was 19.4-times higher than that of $KaiB_{WT}$ (0.5 nM, 1.0 nM, 2.0 nM, 5.0 nM, and 10 nM) (Table 4), indicating that the $KaiB_{10–108}$-$KaiC_{DD}{}^{6mer}$ association was 19.4-times stronger than the $KaiB_{WT}$-$KaiC_{DD}{}^{6mer}$ association. For the interaction with $KaiC_{DD}{}^{6mer}$, the K_A value of $KaiB_{10–108}$ was 2.7-times higher than that of $KaiB_{1–94}$ and 3.9-times higher than that of $KaiB_{10–108}$ incubated at 40 °C for 2 h (“preincubated

$KaiB_{10–108}$," a dimer) (Table 4). Thus, the $KaiB_{10–108}$-$KaiC_{DD}{}^{6mer}$ association was 2.7- and 3.9-times stronger than the $KaiB_{1–94}$-$KaiC_{DD}{}^{6mer}$ and "preincubated $KaiB_{10–108}$"-$KaiC_{DD}{}^{6mer}$ associations, respectively. At a concentration of 4.0 μM at 4 °C, $KaiB_{WT}$ was a mixture of dimer and tetramer, $KaiB_{10–108}$ was a monomer, and $KaiB_{1–94}$ was a dimer (Table 2). Thus, these results suggest that the $KaiB^{1mer}$-$KaiC_{DD}$ and $KaiB^{2mer}$-$KaiC_{DD}$ associations were stronger than the $KaiB^{4mer}$-$KaiC_{DD}$ association.

Stoichiometries of the $KaiB_{10–108}$-$KaiC_{DD}{}^{6mer}$, $KaiB_{1–94}$-$KaiC_{DD}{}^{6mer}$, and $KaiB_{WT}$-$KaiC_{DD}{}^{6mer}$ complexes

I determined the stoichiometries of the $KaiB_{10–108}$-$KaiC_{DD}{}^{6mer}$ complexes formed at 4 °C and 40 °C using GFC at 4 °C. Mixtures containing 20 μM $KaiB_{10–108}$ and 1 μM $KaiC_{DD}{}^{6mer}$ were incubated at 4 °C or 40 °C for 20 h and then subjected to GFC at 4 °C. I collected fractions containing $KaiB_{10–108}$-$KaiC_{DD}{}^{6mer}$ complexes and estimated the amounts of $KaiB_{10–108}$ and $KaiC_{DD}{}^{6mer}$ present in the complexes with SDS-PAGE followed by densitometry. When the $KaiB_{10–108}$-$KaiC_{DD}{}^{6mer}$ complex was formed at 4 °C, the fraction contained 3.1 ± 0.2 subunits of $KaiB_{10–108}$ per molecule of $KaiC_{DD}{}^{6mer}$ (Fig. 5), indicating that the $KaiB_{10–108}$-$KaiC_{DD}{}^{6mer}$ complex formed at 4 °C consisted of three $KaiB_{10–108}$ subunits and one molecule of $KaiC_{DD}{}^{6mer}$. On the other hand, when the complex was formed at 40 °C, the fraction contained 5.6 ± 0.6 subunits of $KaiB_{10–108}$ per molecule of $KaiC_{DD}{}^{6mer}$ (Fig. 5), indicating that the $KaiB_{10–108}$-$KaiC_{DD}{}^{6mer}$ complex formed at 40 °C consisted of five or six

$KaiB_{10–108}$ subunits and one molecule of $KaiC_{DD}{}^{6mer}$.

I also determined the stoichiometries of the $KaiB_{WT}$-$KaiC_{DD}{}^{6mer}$ and $KaiB_{1–94}$-$KaiC_{DD}{}^{6mer}$ complexes formed at 4 °C and 40 °C. $KaiB_{WT}$-$KaiC_{DD}{}^{6mer}$ and $KaiB_{1–94}$-$KaiC_{DD}{}^{6mer}$ complexes formed at 4 °C contained 2.8 ± 0.2 subunits of $KaiB_{WT}$ per molecule of $KaiC_{DD}{}^{6mer}$ (Fig. 5) and 3.3 ± 0.3 subunits of $KaiB_{1–94}$ per molecule of $KaiC_{DD}{}^{6mer}$ (Fig. 5), respectively. These results indicate that the $KaiB_{WT}$-$KaiC_{DD}{}^{6mer}$ and $KaiB_{1–94}$-$KaiC_{DD}{}^{6mer}$ complexes formed at 4 °C consisted of about three KaiB subunits and one molecule of $KaiC_{DD}{}^{6mer}$. On the other hand, the $KaiB_{WT}$-$KaiC_{DD}{}^{6mer}$ and $KaiB_{1–94}$-$KaiC_{DD}{}^{6mer}$ complexes formed at 40 °C contained 4.8 ± 0.3 subunits of $KaiB_{WT}$ per molecule of $KaiC_{DD}{}^{6mer}$ (Fig. 5) and 5.0 ± 0.5 subunits of $KaiB_{1–94}$ per molecule of $KaiC_{DD}{}^{6mer}$, respectively (Fig. 5). These results indicate that the stoichiometries of the KaiB-$KaiC^{6mer}$ complexes were affected by temperature, with the amount of KaiB greater at 40 °C than at 4 °C. To determine the stoichiometries of the KaiB-$KaiC_{DD}{}^{6mer}$ complexes formed at 40 °C, I formed the complexes at 40 °C and then isolated them at 4 °C using GFC. Consequently, the number of KaiB subunits per molecule of $KaiC_{DD}{}^{6mer}$ in the KaiB-$KaiC_{DD}{}^{6mer}$ complexes formed at 40 °C was underestimated because some of KaiC-associated KaiB molecules likely dissociated from the KaiB-$KaiC_{DD}$ complexes during isolation of the complexes by GFC at 4 °C. Thus, the KaiB-$KaiC^{6mer}$ complexes formed at 40 °C likely consisted of six KaiB subunits and one molecule of $KaiC_{DD}{}^{6mer}$.

Effects of temperature on the ATPase activities of KaiC

ATP hydrolysis by the N-terminal ATPase motifs of KaiC is responsible for KaiB-KaiC^{6mer} complex formation (34). Thus, the increase in the number of KaiB subunits associated with KaiC$_{DD}$^{6mer} at 40 °C could be caused by an increase in the ATPase activity of the N-terminal ATP motifs of KaiC$_{DD}$ at the higher temperature though the ATPase activity of KaiC is temperature-compensated in a temperature range between 25 °C and 50 °C (20). Therefore, I assayed the ATPase activities of KaiC$_{WT}$ and KaiC$_{DD}$ at 4 °C, 15 °C, 25 °C, and 40 °C. The ATPase activities of KaiC$_{WT}$ and KaiC$_{DD}$ were almost temperature-compensated in a temperature range between 25 °C and 40 °C (Fig. 6). The Q_{10} values of KaiC$_{WT}$ and KaiC$_{DD}$ between 25 °C and 40 °C were 1.10 ± 0.04 and 1.05 ± 0.02, respectively. On the other hand, the ATPase activities of KaiC$_{WT}$ and KaiC$_{DD}$ increased with temperature increases in a temperature range between 4 °C and 25 °C (Fig. 6) with Q_{10} values of 1.69 ± 0.02 and 1.47 ± 0.01, respectively.

Circadian oscillations in the phosphorylation level of KaiC in an *in vitro* reconstituted KaiABC clock oscillator containing KaiB$_{10–108}$

KaiB$_{1–94}$ (a dimeric mutant) is able to drive normal clock oscillation in an *in vitro* reconstituted KaiABC clock oscillator (1, 12). To determine whether KaiB$_{10–108}$ is able to drive normal clock oscillation in the *in vitro* clock oscillator, I examined circadian oscillations in the phosphorylation level of KaiC in the *in vitro* clock oscillator. When KaiB$_{10–108}$ (3.0 μM) was used in place of KaiB$_{WT}$ or KaiB$_{1–94}$, the circadian oscillations at 25 °C were similar to those observed with KaiB$_{WT}$ or

$KaiB_{1–94}$ (Fig. 7A), indicating that $KaiB_{10–108}$ (probably a mixture of mainly monomer and partly dimer at 25 °C; Fig. 4E) was able to generate normal clock oscillations *in vitro*, similar to $KaiB_{WT}$ (probably a mixture of tetramer and dimer; Fig. 4A and D) and $KaiB_{1–94}$ (a dimer; Fig. 4B and Table 1) (1).

Circadian gene expression rhythms in *T. elongatus* cells

I examined $KaiB_{10–108}$-driven circadian gene expression rhythms in *T. elongatus* cells at 41 °C, using a high-sensitivity bioluminescence monitoring apparatus (Onai *et al*. unpublished). The *kaiB*-null host cells carrying the $kaiB_{WT}$ gene, reintroduced as a positive control, showed normal circadian bioluminescence rhythms, as described previously (1, 32). On the other hand, in cells carrying the $kaiB_{10–108}$ gene, the amplitude of the bioluminescence rhythms was greatly reduced when compared with those in cells carrying the $kaiB_{1–94}$ gene (Fig. 7B) (1). Most of the cells carrying $kaiB_{10–108}$ (10/12 samples) showed arrhythmic bioluminescence. Two KaiB oligomeric structure mutants $KaiB_{10–108}$ and $KaiB_{1–94}$ were able to drive normal clock oscillation *in vitro* as described above (Fig. 7A). Thus, the oligomeric structure of KaiB probably affected the output of the clock oscillation signal from the KaiABC clock oscillator, as described previously (1).

Inhibition of $KaiC_{DD}$-SasA complex formation by $KaiB_{10–108}$

As described above, the oligomeric structure of $KaiB_{10–108}$ as a monomer or a dimer can be

controlled by temperature. Previously, I showed that $KaiB_{1–94}$ (a dimer) inhibited $KaiC_{DD}$-SasA complex formation, whereas $KaiB_{WT}$ (a tetramer) had little effect (1). $KaiB_{1–94}$ associates with $KaiC^{6mer}$ more strongly than does $KaiB_{WT}$ to inhibit the normal interaction of $KaiC^{6mer}$ with SasA (1). To determine the effects of the oligomeric structure of KaiB on the inhibition of $KaiC_{DD}$-SasA complex formation, I used GFC to examine $KaiC_{DD}$-SasA complex formation in the presence of $KaiB_{10–108}$ (Fig. 8B). Reaction mixtures containing 1.5 μM SasA and 0.75 μM $KaiC_{DD}{}^{6mer}$ were incubated at 25 °C for 6 h in the absence or presence of 12 μM $KaiB_{WT}$ (a tetramer under these conditions; Fig. 4A and 3D), $KaiB_{1–94}$ (a dimer; Fig. 4B and Table 1), $KaiB_{10–108}$ (probably a mixture of dimer and monomer; Fig. 2F and 3E), or "preincubated $KaiB_{10–108}$" (a mixture of mainly dimer and partly monomer; Fig. 2F) and then subjected to GFC at 4 °C. The elution profile of the negative control sample, without KaiB, showed three peaks corresponding to a larger form of the $KaiC_{DD}$-SasA complex, a smaller form of the complex, and SasA, respectively (Fig. 8A). On the other hand, the elution profile of the sample with $KaiB_{WT}$ or $KaiB_{1–94}$ as positive controls showed four peaks corresponding to the $KaiC_{DD}$-SasA complex, $KaiC_{DD}$ and the KaiB-$KaiC_{DD}{}^{6mer}$ complex, SasA, and KaiB, respectively (Fig. 8B). The sample with $KaiB_{1–94}$ contained less $KaiC_{DD}$-SasA complex than did the sample with $KaiB_{WT}$ (Fig. 8B), as described previously (1). The elution profile of the sample with $KaiB_{10–108}$ showed four peaks corresponding to $KaiC_{DD}{}^{6mer}$ and the KaiB-$KaiC_{DD}{}^{6mer}$ complex, SasA, one form of $KaiB_{10–108}$ (probably a dimer; "$KaiB_{10–108}{}^{2mer}$"), and another form of $KaiB_{10–108}$ (probably a monomer; "$KaiB_{10–108}{}^{1mer}$"), respectively (Fig. 8B). The

presence of $KaiB_{10–108}$ eliminated the $KaiC_{DD}$-SasA complex and increased the amount of free SasA (Fig. 8B). Thus, $KaiB_{10–108}$ inhibited $KaiC_{DD}$-SasA complex formation to a greater extent than did $KaiB_{1-94}$. The elution profile of the sample with "preincubated $KaiB_{10–108}$" showed five peaks corresponding to the $KaiC_{DD}$-SasA complex, $KaiC_{DD}{}^{6mer}$ and the KaiB-$KaiC_{DD}{}^{6mer}$ complex, SasA, "$KaiB_{10–108}{}^{2mer}$," and "$KaiB_{10–108}{}^{1mer}$," respectively (Fig. 8B). Greater amounts of the $KaiC_{DD}$-SasA complex and "$KaiB_{10–108}{}^{2mer}$" were present in the sample with "preincubated $KaiB_{10–108}$" than in the sample with $KaiB_{10–108}$ (Fig. 8B), indicating that $KaiB_{10–108}$ without preincubation (a monomer before reaction) inhibited $KaiC_{DD}$-SasA complex formation to a greater extent than did "preincubated $KaiB_{10–108}$" (a dimer before reaction). Although the oligomeric structure of $KaiB_{10–108}$ might change during incubation at 25 °C, these results suggest that the inhibitory effects of $KaiB_{10–108}{}^{1mer}$ were stronger than those of $KaiB_{10–108}{}^{2mer}$. This conclusion is consistent with the results obtained with SPR analysis, described above (Table 4).

Discussion

KaiB has an unusual homotetrameric structure comprising two asymmetric dimers, as shown by crystallography (31-33). However, by analyzing $KaiB_{1–94}$, a dimeric KaiB mutant, it has been demonstrated that $KaiB_{WT}$ might exist as $KaiB_{WT}{}^{2mer}$ in the KaiB-$KaiC^{6mer}$ complex (1). Does $KaiB_{WT}$ exist mainly as a monomer, a dimer or a tetramer *in vitro* and in cyanobacterial cells? $KaiB_{10–108}$ existed in equilibrium between $KaiB_{10–108}{}^{1mer}$ and $KaiB_{10–108}{}^{2mer}$, depending on the temperature (Fig. 2F and Table 1). At low KaiB concentrations (4.0 μM) or at high NaCl concentrations (1 M), $KaiB_{WT}{}^{4mer}$ partially dissociated into $KaiB_{WT}{}^{2mer}$ (Fig. 4A and F). Using previously reported data on the number of KaiB molecules in a cyanobacterial cell (35) and assuming a cell size of 100 μm^3 ($\varnothing$ = 3.98 μm, l = 10 μm) (23), I calculated the concentration of KaiB expressed as monomer concentration in the cell to be 0.13–0.44 μM, which is close to the concentration range of 0.35–20 μM expressed as monomer concentration within which circadian oscillation occurs *in vitro* (14) (Mutoh *et al*. unpublished data). These values for the intracellular KaiB concentration are lower than 4.0 μM , at which KaiB existed as a mixture of $KaiB^{2mer}$ and $KaiB^{4mer}$ *in vitro* (Fig. 4A and Table 2). Thus, $KaiB^{2mer}$, as well as $KaiB^{4mer}$, is likely present in cyanobacterial cells. At much lower KaiB concentrations, $KaiB^{1mer}$ would also be present in the cells, and KaiB would exist in equilibrium between $KaiB^{1mer}$, $KaiB^{2mer}$, and $KaiB^{4mer}$ (Fig. 9A). Previously, it has been demonstrated using site-directed spin-labeling electron spin resonance analysis that incubation at 40 °C induces the relaxation of the dimer-dimer interface of the $KaiB^{4mer}$ molecule (24).

Thus, the oligomeric structure of $KaiB_{WT}$, as well as that of $KaiB_{10–108}$, could depend on the temperature. However, I did not detect temperature-dependent oligomeric structure changes in $KaiB_{WT}$ under the conditions examined (4 °C and 40 °C) (Fig. 4D and Table1). Temperature would mainly affect the equilibrium between $KaiB^{1mer}$ and $KaiB^{2mer}$ (Fig. 9A), although higher temperatures, such as 40 °C, induce the relaxation of the dimer-dimer interface of $KaiB^{4mer}$ (24).

Here, I showed that the KaiB-$KaiC_{DD}{}^{6mer}$ complexes (containing $KaiB_{WT}$, $KaiB_{1–94}$, or $KaiB_{10–108}$) that formed at 4 °C consisted of three KaiB subunits per molecule of $KaiC_{DD}$ (Fig. 5). On the other hand, the KaiB-$KaiC_{DD}$ complexes (containing $KaiB_{WT}$, $KaiB_{1–94}$, or $KaiB_{10–108}$) that formed at 40 °C consisted of six KaiB subunits per molecule of $KaiC_{DD}{}^{6mer}$ (Fig. 5). Previously, it has been determined the stoichiometries of the KaiB-$KaiC_{DD}{}^{6mer}$ complexes (containing $KaiB_{WT}$ or $KaiB_{1–94}$) that formed at 40 °C and proposed that the complexes contained four KaiB subunits per molecule of $KaiC_{DD}{}^{6mer}$ (1). I re-examined previous data (1) and found that the KaiB-$KaiC_{DD}{}^{6mer}$ complexes that formed at 40 °C contained about six KaiB subunits per molecule of $KaiC_{DD}{}^{6mer}$ (data not shown). Consistently, a similar stoichiometry for the KaiB-$KaiC^{6mer}$ complex has been proposed based on data obtained from single particle analysis of the cryo-electron microscopy images of the KaiB-$KaiC^{6mer}$ complex (51).

Which oligomer of KaiB—monomer, dimer or tetramer—is present in the KaiB-$KaiC_{DD}$ complexes (containing $KaiB_{WT}$, $KaiB_{1–94}$ or $KaiB_{10–108}$)? At 4 °C, $KaiB_{10–108}$ was a monomer (Table 1), suggesting that $KaiB_{10–108}$ is present as a monomer in the $KaiB_{10–108}$-$KaiC_{DD}{}^{6mer}$ complex formed

at 4 °C. If so, $KaiC_{DD}^{6mer}$ should have three $KaiB_{10–108}^{1mer}$-binding sites at 4 °C. $KaiB_{WT}$, $KaiB_{1–94}$, and $KaiB_{10–108}$ likely bind to the same binding sites on $KaiC_{DD}^{6mer}$. If so, each of the three $KaiB_{WT}$ or $KaiB_{1–94}$ subunits should bind to one of the three $KaiB^{1mer}$-binding sites on $KaiC_{DD}^{6mer}$ at 4 °C. Upon interaction with $KaiC_{DD}^{6mer}$ at 4 °C, $KaiB_{WT}$ and $KaiB_{1–94}$ would dissociate into $KaiB_{WT}^{1mer}$ and $KaiB_{1–94}^{1mer}$, respectively, and each of the three $KaiB_{WT}^{1mer}$ or $KaiB_{1–94}^{1mer}$ molecules would bind to one of the three $KaiB^{1mer}$-binding sites on $KaiC_{DD}^{6mer}$. However, I have not yet detected $KaiB_{WT}^{1mer}$ and $KaiB_{1–94}^{1mer}$ experimentally. On the other hand, at 40 °C, $KaiB_{10–108}$ was a dimer (Fig. 2F and Table 1), suggesting that $KaiB_{10–108}$ is also present as a dimer in the complex formed at 40 °C. If this is the case, $KaiC_{DD}^{6mer}$ should have three $KaiB^{2mer}$-binding sites at 40 °C, and three molecules of $KaiB_{10–108}^{2mer}$ would associate with one molecule of $KaiC_{DD}^{6mer}$ at 40 °C. The other possibility is that $KaiC_{DD}^{6mer}$ has six $KaiB^{1mer}$-binding sites at 40 °C: upon interacting with $KaiC_{DD}^{6mer}$ at 40 °C, three $KaiB_{10–108}^{2mer}$ molecules dissociate into six $KaiB_{10–108}^{1mer}$ molecules and bind to six $KaiB^{1mer}$-binding sites on $KaiC_{DD}^{6mer}$. ATP hydrolysis by the N-terminal ATPase motifs of KaiC is responsible for KaiB-$KaiC^{6mer}$ complex formation (34). Therefore, when the ATPase activity of the N-terminal ATPase motifs increases, the number of KaiB binding sites on KaiC should increase. The increase in the ATPase activity of the N-terminal ATP motifs of $KaiC_{DD}$ at 40 °C (Fig. 6) would explain the increase in the number of KaiB subunits associated with $KaiC_{DD}^{6mer}$ at 40 °C (Fig. 5). A model for the oligomeric structure changes of KaiB and for its association with $KaiC^{6mer}$ wherein, upon interaction with $KaiC^{6mer}$ at 40 °C, KaiB dissociates into monomers, and the

six monomers associate with one molecule of $KaiC^{6mer}$ is proposed (Fig. 9A). However, it is uncertain how many molecule of $KaiB^{1mer}$ actually associates with one molecule of $KaiC^{6mer}$ in cyanobacterial cells.

The amounts of KaiB and KaiC in the cells have been reported to change rhythmically, with a molecular ratio of KaiB subunit : KaiC subunit = 2:1 during the circadian cycle (35). Thus, $KaiB^{1mer}$ is able to occupy all the six KaiB-binding sites of all the $KaiC^{6mer}$ contained in the cells. At low KaiB concentrations, KaiB exists as $KaiB^{1mer}$ with high KaiC-binding affinity, and therefore, all the six KaiB-binding sites of $KaiC^{6mer}$ would be occupied with $KaiB^{1mer}$. On the other hand, at high KaiB concentrations, KaiB exists as $KaiB^{4mer}$ with low KaiC-binding affinity, and therefore, all the six KaiB-binding sites of $KaiC^{6mer}$ may not be occupied with $KaiB^{1mer}$ at once. Thus, the number of $KaiB^{1mer}$ in $KaiB^{1mer}$-$KaiC^{6mer}$ complex would oscillate circadianly, and the extent of the competitive inhibition of $KaiC^{6mer}$-SasA interaction would also oscillate circadianly.

$KaiB_{10–108}$ was able to drive normal clock oscillation in the *in vitro* KaiABC clock oscillator (Fig. 7A), similar to $KaiB_{1–94}$ (1). Thus, it is likely that $KaiB_{10–108}$ and $KaiB_{1–94}$ can generate normal clock oscillation *per se* in cyanobacterial cells. However, cyanobacterial cells expressing $KaiB_{10–108}$ on a Δ*kaiB* genetic background showed greatly weakened circadian gene expression rhythms (Fig. 7B), as did cells expressing $KaiB_{1–94}$ (1, 32). Therefore, I conclude that the tetramer structure of KaiB is critical for the generation of circadian gene expression rhythms in cyanobacterial cells (Fig. 9B and C). However, it is possible that the N-terminal and C-terminal sequences deleted from

$KaiB_{10–108}$ and $KaiB_{1–94}$, respectively, are both required for the generation of the circadian gene expression rhythms in the cells. In the KaiB crystal structure, N-terminal amino acids 1–14 and C-terminal amino acids 88–108 are found at the dimer-dimer interface (32). Both $KaiB_{1–94}$ and $KaiB_{10–108}$ existed as native proteins (Fig. 3), and they were able to drive normal clock oscillation in the *in vitro* KaiABC clock oscillator (Fig. 7A). Neither $KaiB_{1–94}$ nor $KaiB_{10–108}$ formed a tetramer under the conditions examined (Table 1 and 2) (1). Therefore, both the C-terminal (95–108) and N-terminal (1–9) sequences of KaiB are required for KaiB tetramer formation, which is critical for the generation of circadian gene expression rhythms in cyanobacterial cells (Fig. 9B and C).

SasA, a KaiC-binding histidine kinase in the SasA-RpaA two-component regulatory system in cyanobacteria, is involved in the main clock output pathway in cyanobacteria (6, 7). Ultimately, the time information of the KaiABC clock oscillator is transmitted to the transcription apparatus to generate genome-wide circadian transcription rhythms in cyanobacterial cells (6, 7, 36). Association of KaiC with SasA is the first step in the SasA-mediated clock output pathway (1), and the association of KaiB with KaiC competitively inhibits the SasA-KaiC complex formation (1). Previously, it has been hypothesized that inhibition of normal KaiC-SasA complex formation by $KaiB_{1–94}$ causes the defect in circadian gene expression rhythms observed in cyanobacterial cells expressing $KaiB_{1–94}$ on a Δ*kaiB* genetic background. Similarly, cyanobacterial cells expressing $KaiB_{10–108}$ on a Δ*kaiB* genetic background exhibited a defective rhythm phenotype (Fig. 7B), and $KaiB_{10–108}$, to a greater extent than $KaiB_{WT}$ (a tetramer; Fig. 8B), inhibited $KaiC_{DD}$-SasA complex

formation (Fig. 8B). I conclude that stronger inhibitions of KaiC-SasA complex formation by $KaiB_{10–108}$ (a mixture of a monomer and dimer; Fig. 8B) and $KaiB_{1–94}$ (a dimer; Fig. 8B) than that by $KaiB_{WT}$ (a tetramer; Fig. 8B) caused the defective rhythm phenotype in cyanobacterial cells expressing $KaiB_{10–108}$ or $KaiB_{1–94}$ on a Δ*kaiB* genetic background (Fig. 9B and C). As described previously (1), oligomeric structure changes in KaiB are likely critical for the generation of circadian gene expression rhythms in cyanobacterial cells *via* the regulation of the KaiC-SasA interaction by KaiB (Fig. 9B and C).

On one surface of the $KaiB^{4mer}$ molecule, a PC, the active site, is covered with two NRs. Upon interaction with KaiC, a positively charged region (PR) that forms the PC may be exposed to solvent to facilitate the association of KaiB with KaiC (Fig. 9A). Previously, it has been proposed two related models. In the first, NR movement exposes the PC for ligand binding (32). In the second, dimerization of KaiB exposes the PR (1). $KaiB_{1–94}$ (a dimer), which lacks the NRs and whose PR is exposed to solvent, had a higher affinity for $KaiC_{DD}{}^{6mer}$ than did $KaiB_{WT}$ (Table 4) (1). This result is consistent with either model. $KaiB_{10–108}$, which has NRs, had a higher affinity for $KaiC_{DD}$ than did $KaiB_{1–94}$ (a dimer) and "preincubated $KaiB_{10–108}$" (a dimer) (Table 4). This result suggests that the dissociation of $KaiB^{4mer}$ into dimers and monomers exposes the PR and that the KaiB monomerization, rather than dimerization, is more efficient for exposing the PR (Fig. 9A).

Although I have not yet detected $KaiB_{WT}{}^{1mer}$ under the conditions examined, my findings suggest that KaiB exists in equilibrium between a monomer, dimer, and tetramer in cyanobacterial

cells. Sedimentation velocity analysis may be effective to detect $KaiB_{WT}{}^{1mer}$ and equilibrium between $KaiB_{WT}{}^{1mer}$, $KaiB_{WT}{}^{2mer}$, and $KaiB_{WT}{}^{4mer}$. The $KaiC_{DD}{}^{6mer}$-binding affinity of $KaiB_{10\text{-}108}$ changed depending on temperature *via* the oligomeric structure changes of $KaiB_{10\text{-}108}$ (Table 4). This finding is interesting in relation to the temperature compensation of the period length of the cyanobacterial circadian clock oscillator. Detailed SPR analysis of the $KaiC_{DD}{}^{6mer}$-binding affinity of KaiB ($KaiB_{WT}$ and $KaiB_{10\text{-}108}$) performed at various temperatures will reveal the relation between the $KaiC_{DD}{}^{6mer}$-binding affinity of KaiB and temperature. It is not easy to study the role of each oligomeric structure of KaiB in detail by analyzing available KaiB proteins such as $KaiB_{WT}$, $KaiB_{1\text{-}94}$, and $KaiB_{10\text{-}108}$ because their oligomeric structures change depending on temperature, KaiB ($KaiB_{10\text{-}108}$) concentration ($KaiB_{WT}$, $KaiB_{1\text{-}94}$, and $KaiB_{10\text{-}108}$), and NaCl concentration ($KaiB_{WT}$), which are not controlled freely for the analyses. Therefore, it is necessary to construct three mutant KaiB proteins whose oligomeric structure are a stable monomer, dimer and tetramer, respectively. To obtain a stable $KaiB^{1mer}$, I have already constructed many truncated KaiB mutants with each different N-terminal deletions. To prepare stable $KaiB^{2mer}$ and $KaiB^{4mer}$, the introduction of a disulfide bond into the monomer-monomer interface of $KaiB_{1\text{-}94}$ and disulfide bond introductions into monomer-monomer and dimer-dimer interfaces of $KaiB_{WT}$ would be effective. KaiA and KaiC as well as KaiB are multimers, and thus, they also might exist in equilibriums between different oligomeric structures. It is interesting to know whether KaiA and KaiC also perform oligomeric structure changes depending on temperature and their concentrations and whether their oligomeric

structure changes affect the mutual binding affinities of three Kai proteins. The analysis applied to KaiB could be applied to KaiA and KaiC similarly.

Figures and Tables

Fig. 1

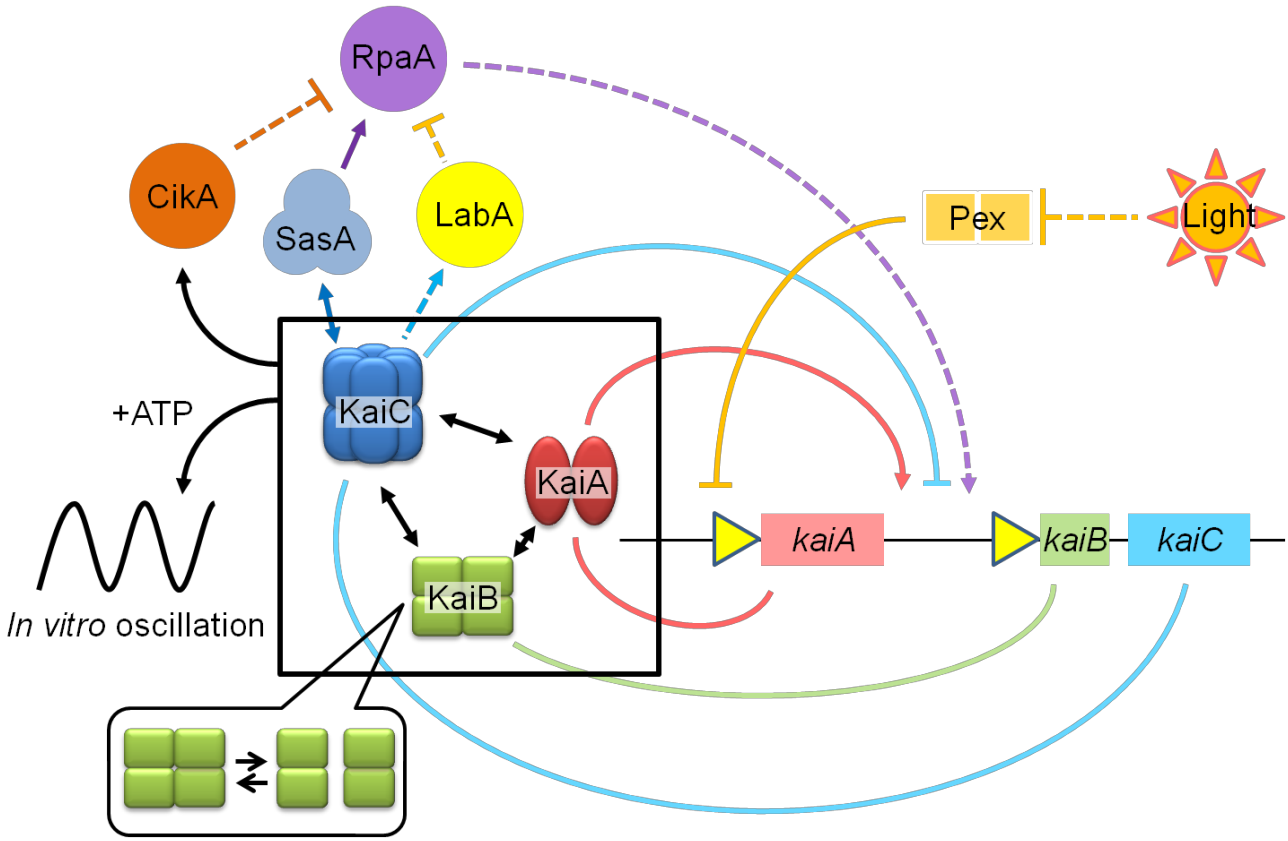
RpaA
CikA
SasA
LabA
Pex
Light
+ATP
KaiC
KaiA
KaiB
kaiA
kaiB
kaiC
In vitro oscillation

Figure 1 A model of the cyanobacterial circadian clock system. Details are described in the text.

Fig. 2

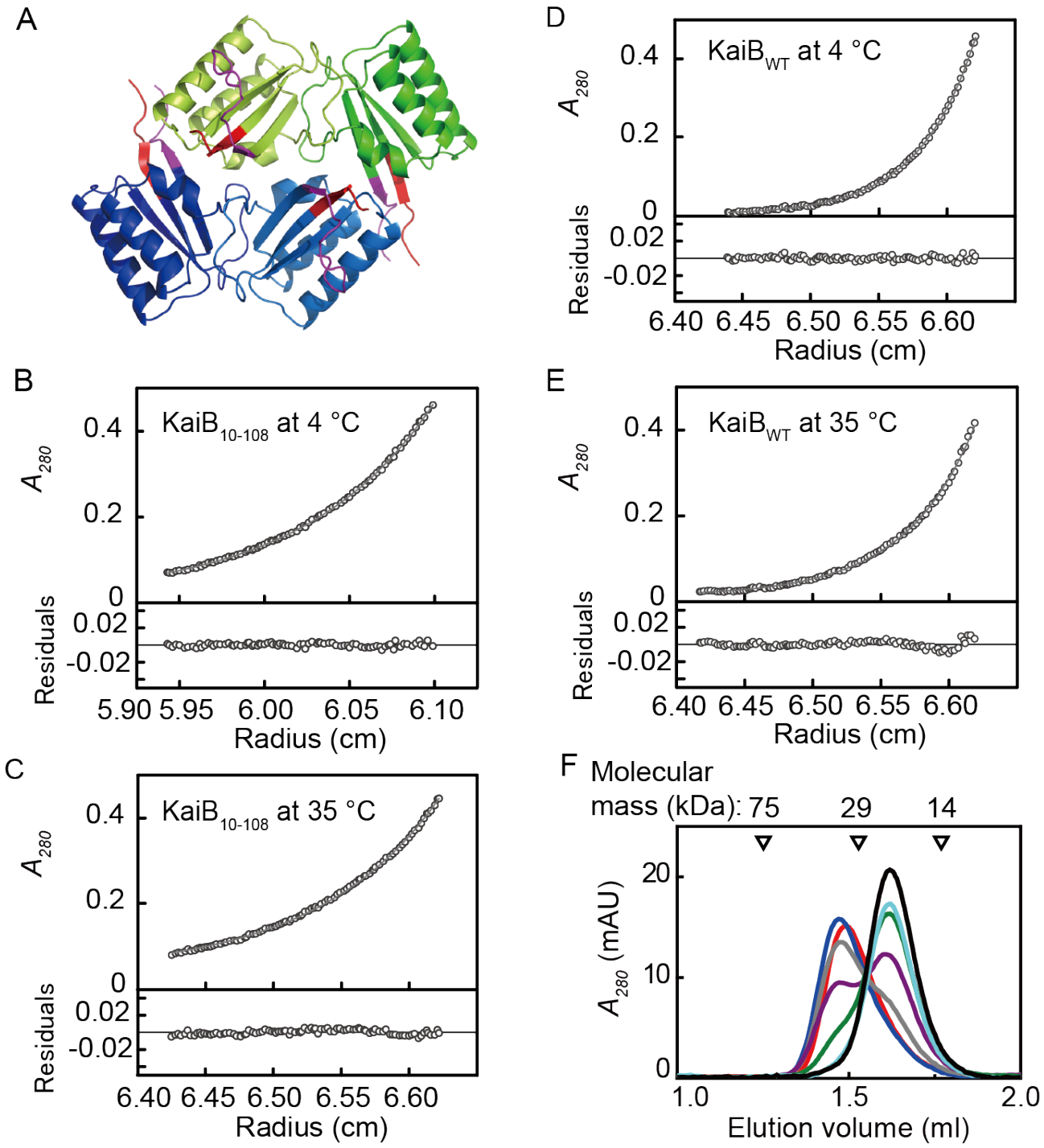
A
B
KaiB10-108 at 4 °C
A280
Residuals
Radius (cm)
C
KaiB10-108 at 35 °C
D
KaiBWT at 4 °C
E
KaiBWT at 35 °C
F
Molecular
mass (kDa): 75 29 14
A280 (mAU)
Elution volume (ml)

Figure 2 Determination of the oligomeric structure of $KaiB_{10–108}$. (A) N-terminal deletion in $KaiB_{10–108}$ and C-terminal deletion in $KaiB_{1–94}$. N-terminal amino acid residues 1 to 9, deleted in $KaiB_{10–108}$, are shown in red, and C-terminal amino acid residues 95 to 108, deleted in $KaiB_{1–94}$, are shown in purple in the crystal structure of the *T. elongatus* KaiB tetramer. (B–E) SE of $KaiB_{10–108}$ and $KaiB_{WT}$. The upper panels show the equilibrium profiles (open circles) displayed as the A_{280} (Au) versus the radial distance and theoretical concentration profiles (solid line) for a single molecular species with molecular masses of 11.4 (B), 22.8 (C), and 49.7 (D and E) kDa, respectively. The lower panels show the residual plots from the curve fitting. B and C, $KaiB_{10–108}$; D and E, $KaiB_{WT}$. Temperature: B and D, 4 °C; C and E, 35 °C. (F) Temperature dependence of the apparent molecular mass of $KaiB_{10–108}$ estimated using GFC. $KaiB_{10–108}$ was incubated at 4 °C, 15 °C, 20 °C, 25 °C, 30 °C, 35 °C, or 40 °C for 6 h and then subjected to analytical GFC on a Superdex 75 5/150GL column (GE Healthcare) equilibrated with reaction buffer at 4 °C. The elution positions of the molecular mass standards conalbumin (75 kDa), carbonic anhydrase (29 kDa), and ribonuclease (14 kDa) are indicated by the arrowheads above the elution profiles. Typical elution profiles from three independent experiments are shown. Temperature: black line, 4 °C; cyan line, 15 °C; green line, 20 °C; purple line, 25 °C; grey line, 30 °C; blue line, 35 °C; red line, 40 °C.

Fig. 3

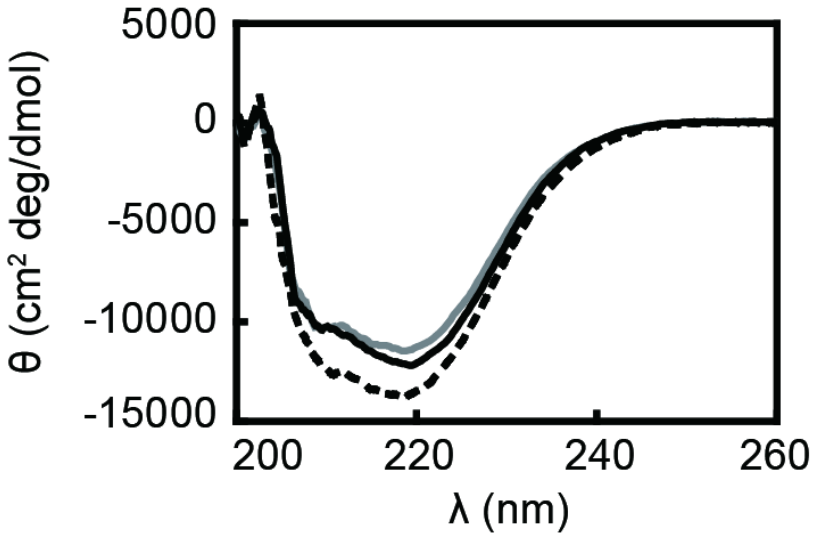

Figure 3 CD spectra of $KaiB_{10–108}$, $KaiB_{WT}$, and $KaiB_{1–94}$. CD spectra of $KaiB_{10–108}$ (black line), $KaiB_{WT}$ (gray line), and $KaiB_{1–94}$ (black broken line) were measured over a wavelength range of 200–260 nm at 4 °C. Typical profiles from three independent experiments are shown.

Fig. 4

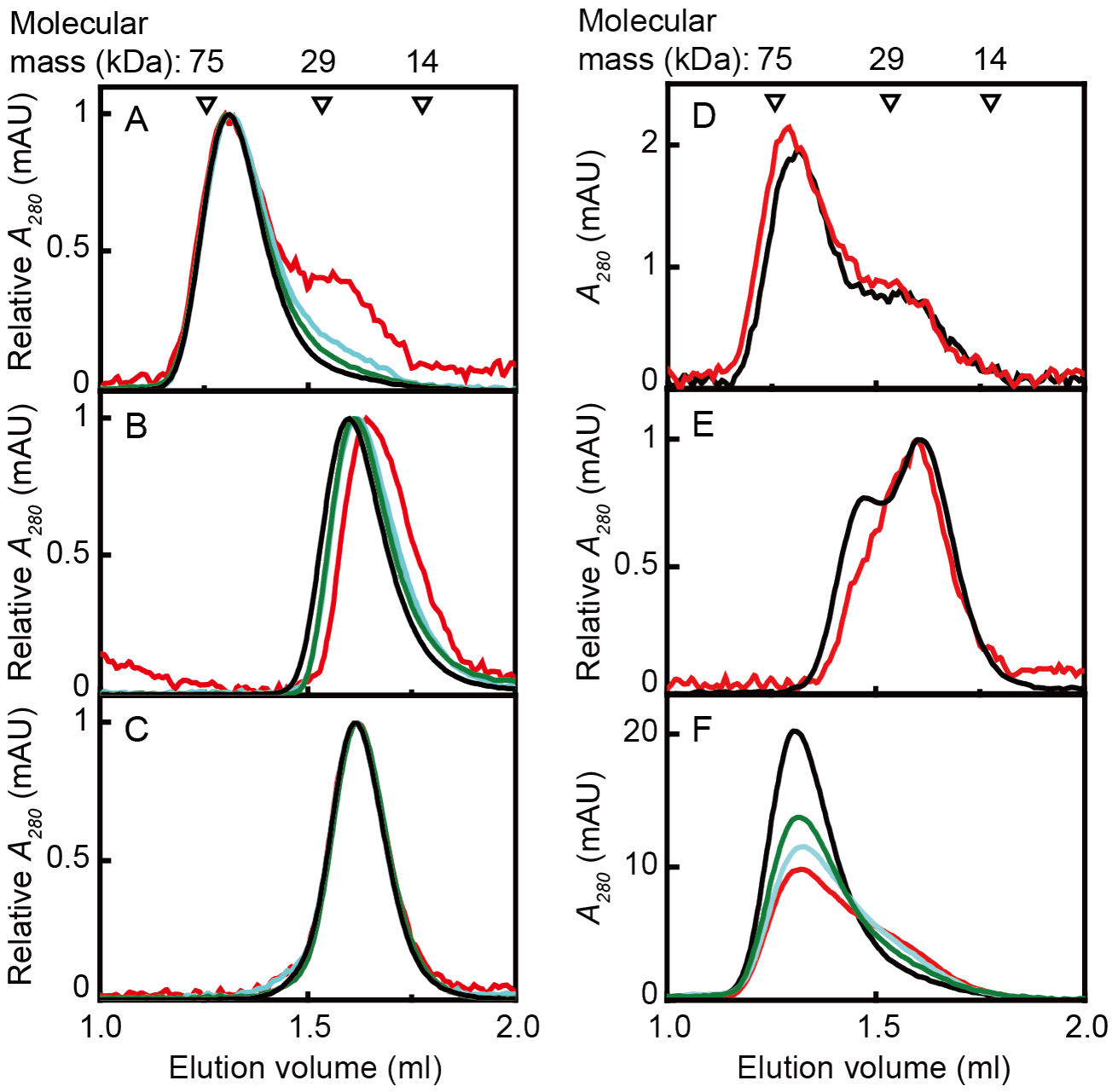
Molecular
mass (kDa): 75
29
14
A
B
C
D
E
F
Relative A_{280} (mAU)
A_{280} (mAU)
Elution volume (ml)
1.0
1.5
2.0

Figure 4 The GFC elution profiles of $KaiB_{10–108}$, $KaiB_{WT}$, and $KaiB_{1–94}$ under various conditions. (A–C) KaiB-concentration dependence. $KaiB_{WT}$ (A), $KaiB_{1–94}$ (B), and $KaiB_{10–108}$ (C) (4.0 μM, 12 μM, 24 μM, and 48 μM) were separately incubated at 4 °C for 6 h and then subjected to analytical GFC at 4 °C as described in the legend for Fig. 2F. Elution profiles representative of three independent experiments are shown as relative values, with peaks being 1. KaiB concentration: black line, 48 μM; green line, 24 μM; cyan line, 12 μM; red line, 4.0 μM. (D) Temperature dependence of $KaiB_{WT}$ at lower concentrations, at which $KaiB_{WT}$ existed as a mixture of tetramer and dimer. $KaiB_{WT}$ (4.0 μM) was incubated at 4 °C or 40 °C for 6 h and then subjected to analytical GFC. Typical elution profiles are shown. Temperature: black line, 4 °C; red line, 40 °C. (E) KaiB-concentration dependence of $KaiB_{10–108}$ at a higher temperature, at which $KaiB_{10–108}$ existed as a mixture of monomer and dimer. $KaiB_{10–108}$ (4.0 μM and 24 μM) was incubated at 25 °C for 6 h and then subjected to analytical GFC. Typical elution profiles are shown as relative values, with peaks being 1. $KaiB_{10–108}$ concentration: black line, 4.0 μM; red line, 48 μM. (F) NaCl-concentration dependence of $KaiB_{WT}$. $KaiB_{WT}$ was incubated in 20 mM HEPES-NaOH buffer (pH 7.5) containing 150 mM, 300 mM, 500 mM, or 1000 mM NaCl at 4 °C for 16 h and then subjected to analytical GFC, using each corresponding buffer as the GFC buffer. Typical elution profiles are shown. NaCl concentration: black line, 150 mM; green line, 300 mM; cyan line, 500 mM; red line, 1000 mM.

Fig. 5

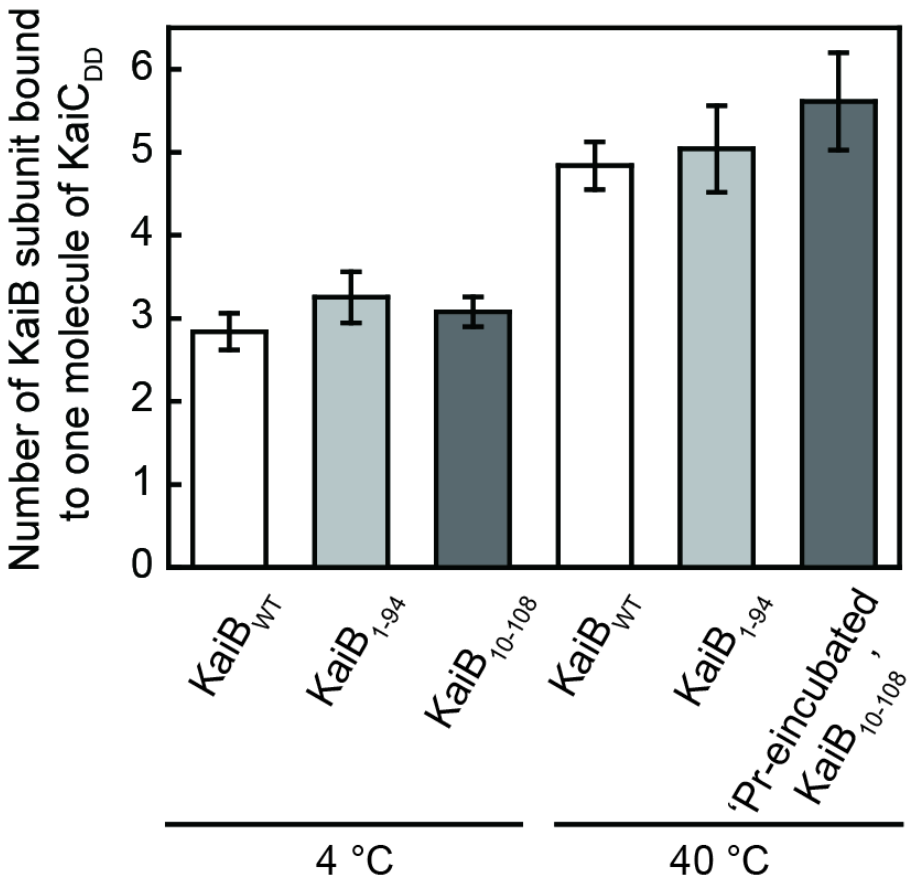
Number of KaiB subunit bound to one molecule of KaiC$_{DD}$
0
1
2
3
4
5
6
KaiB$_{WT}$
KaiB$_{1-94}$
KaiB$_{10-108}$
KaiB$_{WT}$
KaiB$_{1-94}$
'Pr-eincubated' KaiB$_{10-108}$
4 °C
40 °C

Figure 5 Stoichiometries of KaiB-$KaiC_{DD}^{6mer}$ complexes. Reaction mixtures containing 20 μM KaiB ($KaiB_{WT}$, $KaiB_{1–94}$, $KaiB_{10–108}$, or "preincubated $KaiB_{10–108}$") and 1 μM $KaiC_{DD}^{6mer}$ in reaction buffer containing 1 mM ATP and 5 mM $MgCl_2$ were incubated at 4 °C or 40 °C for 20 h and then subjected to GFC at 4 °C. Aliquots of fractions containing KaiB-$KaiC_{DD}^{6mer}$ complexes were subjected to SDS-PAGE. Standard amounts of $KaiB_{WT,}$ $KaiB_{1–94}$, $KaiB_{10–108}$, and $KaiC_{DD}^{6mer}$ were also applied to the gels. I determined the amounts of KaiB and $KaiC_{DD}^{6mer}$ in the complexes using densitometry and calculated the number of $KaiB_{WT}$, $KaiB_{1–94}$, or $KaiB_{10–108}$ subunits per molecule of $KaiC_{DD}^{6mer}$ in the KaiB-$KaiC_{DD}^{6mer}$ complexes. Values are the mean ± SD from three independent experiments.

Fig. 6

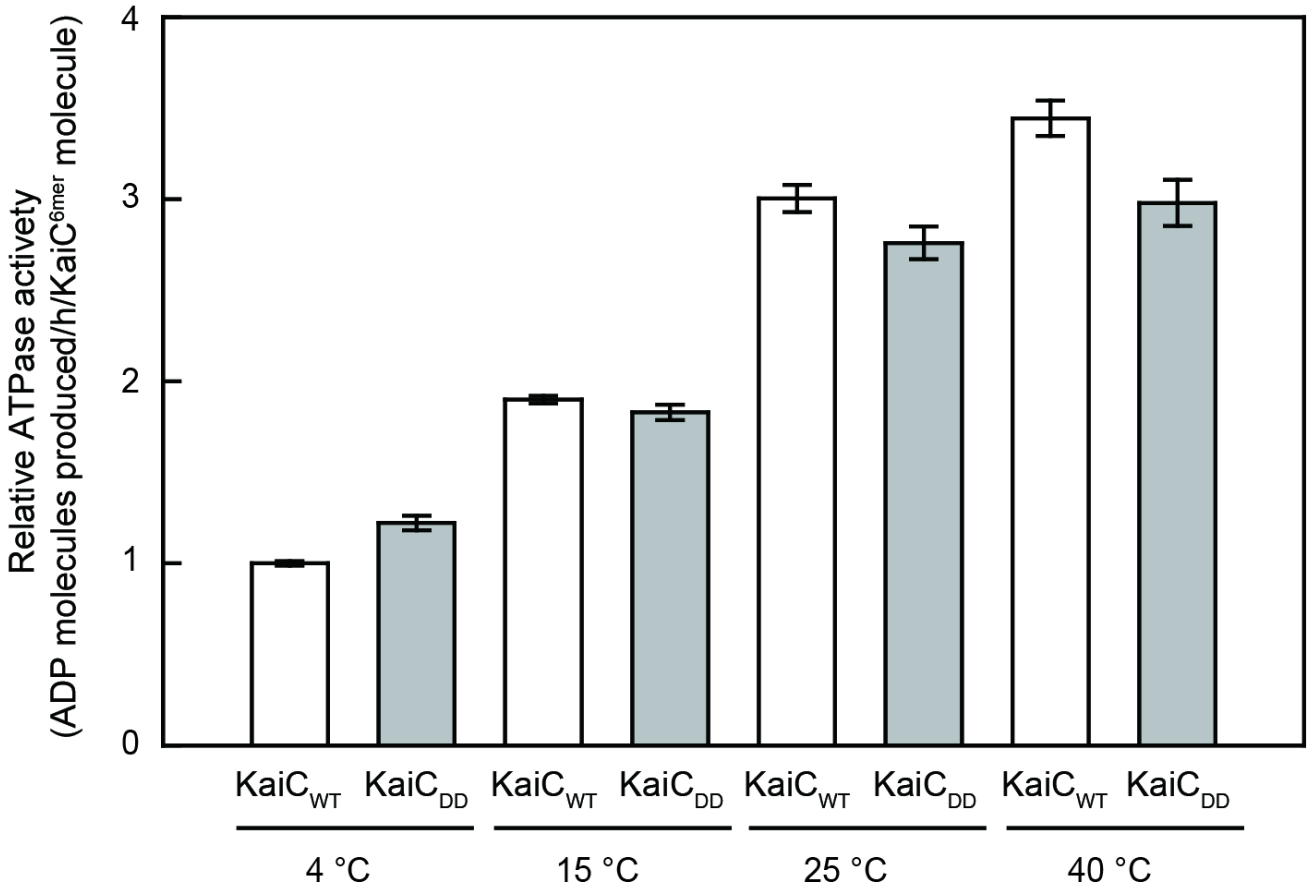
Relative ATPase activety
(ADP molecules produced/h/KaiC6mer molecule)
4
3
2
1
0
KaiCWT
KaiCDD
KaiCWT
KaiCDD
KaiCWT
KaiCDD
KaiCWT
KaiCDD
4 °C
15 °C
25 °C
40 °C

Figure 6 ATPase activities of KaiC at various temperatures. Reaction mixtures containing 1 μM $KaiC^{6mer}$ ($KaiC_{WT}{}^{6mer}$ or $KaiC_{DD}{}^{6mer}$) in reaction buffer containing 1 mM ATP and 5 mM $MgCl_2$ were incubated at 4 °C, 15 °C, 25 °C or 40 °C for 20 h. ATPase activities were then measured. Values are the mean ± SD from three independent experiments.

Fig. 7

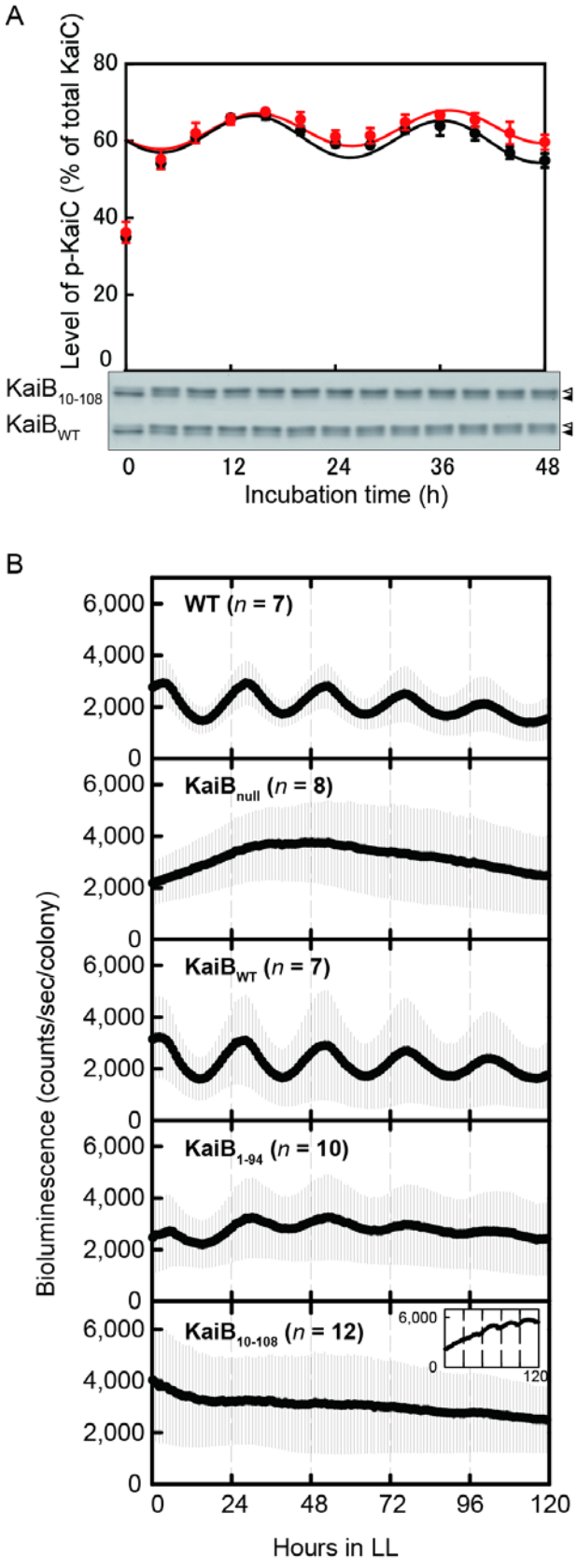

Figure 7 Circadian oscillations driven by KaiB$_{10–108}$. (A) Circadian oscillations in the

phosphorylation level of KaiC in an *in vitro* KaiABC clock oscillator. Reaction mixtures containing 0.75 μM KaiA, 3.0 μM $KaiB_{10–108}$, or $KaiB_{WT}$ and 0.5 μM $KaiC^{6mer}$ in reaction buffer containing 1 mM ATP and 5 mM $MgCl_2$ were incubated at 25 °C for the periods indicated. Aliquots of the reaction mixtures were subjected to SDS-PAGE on 12.5% gels, and the gels were stained with CBB. I estimated the relative amounts of the non phosphorylated form of KaiC (np-KaiC) and the phosphorylated form of KaiC (p-KaiC) with densitometry, calculated the phosphorylation level of KaiC, and analyzed circadian oscillations in the level using the RAP rhythm-analyzing program. The simulated curves are shown (upper panel). Values shown are the mean ± SD from triplicate measurements. KaiB added: red circles, $KaiB_{10–108}$; black circles, $KaiB_{WT}$. Representative photographs of stained gels from triplicate experiments are shown (lower panel). Open arrows, p-KaiC; closed arrows, np-KaiC. (B) Circadian gene expression rhythms in cyanobacterial cells. Bioluminescence rhythms of *T. elongatus* P_{psbA1}::Xl *luxAB* reporter strains carrying $kaiB_{WT}$ ($KaiB_{WT}$, $n = 7$), $kaiB_{1–94}$ ($KaiB_{1–94}$, $n = 10$), $kaiB_{10–108}$ ($KaiB_{10–108}$, $n = 12$), or no additional *kaiB* gene ($KaiB_{null}$, $n = 8$) on a *kaiB*-null background (the *kaiB* gene had a nonsense codon just downstream of its initiation codon). I measured bioluminescence rhythms at 41 °C in constant light after 12 h of darkness. Data points and error bars indicate the mean ± SD from *n* independent samples. I obtained essentially the same results in three independent experiments. cps, counts per s. The inset in the $KaiB_{10–108}$ panel shows the bioluminescence rhythm in the two $KaiB_{10–108}$ samples whose bioluminescence was rhythmic ($n = 2$). Table 5 summarizes the results.

Fig. 8

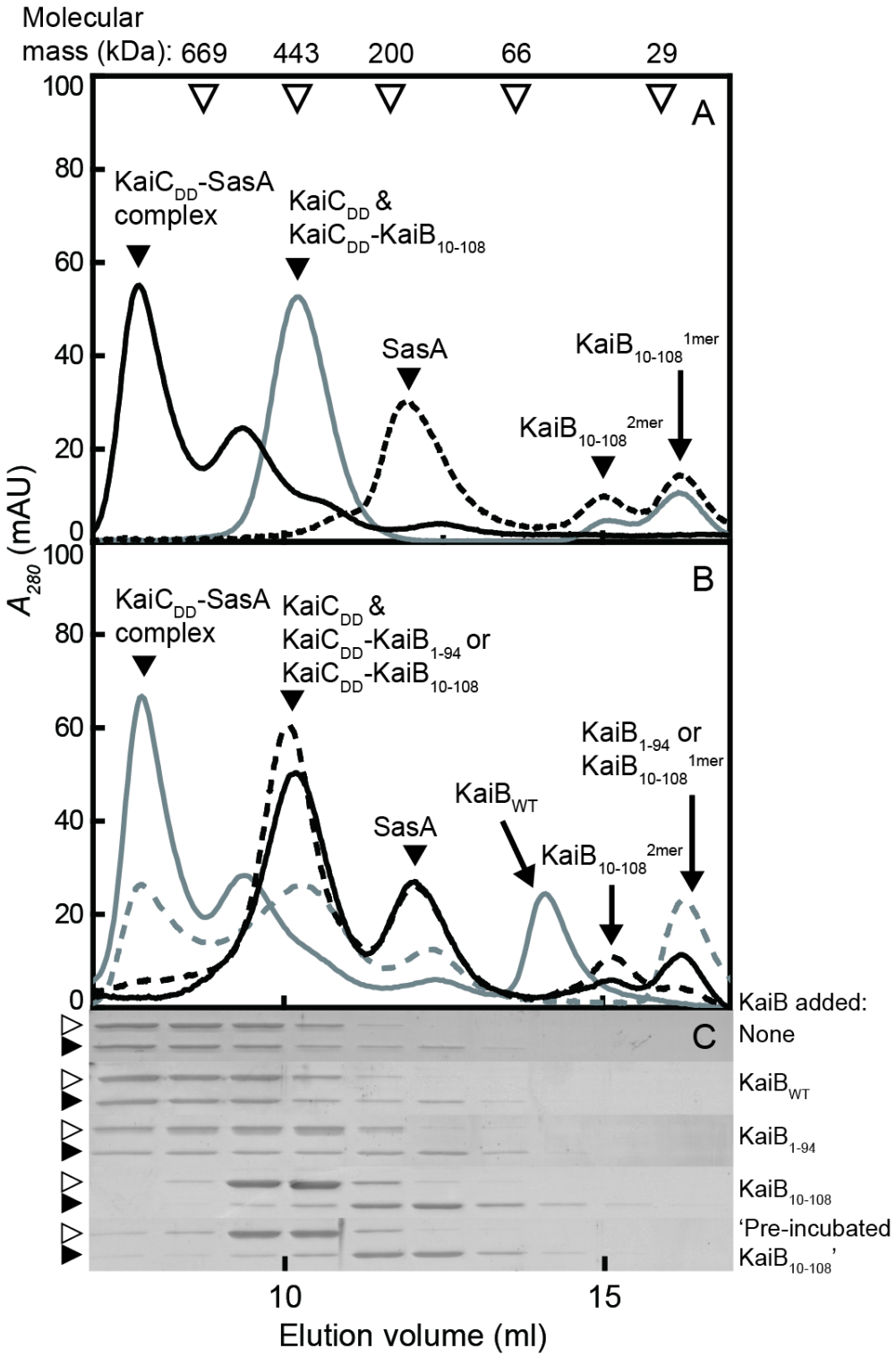
Molecular
mass (kDa): 669 443 200 66 29
A
KaiC$_{DD}$-SasA
complex
KaiC$_{DD}$ &
KaiC$_{DD}$-KaiB$_{10-108}$
SasA
KaiB$_{10-108}$ ^{1mer}
KaiB$_{10-108}$ ^{2mer}
B
KaiC$_{DD}$-SasA
complex
KaiC$_{DD}$ &
KaiC$_{DD}$-KaiB$_{1-94}$ or
KaiC$_{DD}$-KaiB$_{10-108}$
KaiB$_{1-94}$ or
KaiB$_{10-108}$ ^{1mer}
KaiB$_{WT}$
SasA
KaiB$_{10-108}$ ^{2mer}
A_{280} (mAU)
100
80
60
40
20
0
C
KaiB added:
None
KaiB$_{WT}$
KaiB$_{1-94}$
KaiB$_{10-108}$
'Pre-incubated
KaiB$_{10-108}$'
10
15
Elution volume (ml)

Figure 8 Inhibition of $KaiC_{DD}$-SasA complex formation by $KaiB_{10–108}$ assayed with GFC. (A) $KaiB_{10–108}$-$KaiC_{DD}^{6mer}$ complex formation and $KaiC_{DD}$-SasA complex formation. Reaction mixtures containing 0.75 μM $KaiC_{DD}^{6mer}$ and 1.5 μM SasA (black solid line), those containing 0.75 μM $KaiC_{DD}^{6mer}$ and 6 μM $KaiB_{10–108}$ (gray solid line), and those containing 1.5 μM SasA and 6 μM $KaiB_{10–108}$ (black broken line) were separately incubated at 25 °C for 18 h in reaction buffer containing 1 mM ATP, 5 mM $MgCl_2$, and 0.1 mM DTT. To identify the proteins in the chromatography fractions, I analyzed aliquots of fractions with SDS-PAGE and stained the gels with CBB. Typical elution profiles are shown. (B) Inhibition of $KaiC_{DD}$-SasA complex formation by KaiB. Reaction mixtures containing 0.75 μM $KaiC_{DD}^{6mer}$, 1.5 μM SasA, and 12 μM KaiB ($KaiB_{WT}$: gray line, $KaiB_{1–94}$: gray broken line, $KaiB_{10–108}$: black solid line, “preincubated $KaiB_{10–108}$”: black broken line) were incubated and analyzed. (C) Typical photographs of the stained gels. Aliquots of the fractions (elution volumes, 7–17 ml) were subjected to SDS-PAGE on 18% gels, and the gels were visualized with CBB staining. Open and closed arrowheads indicate $KaiC_{DD}$ and SasA, respectively.

Fig. 9

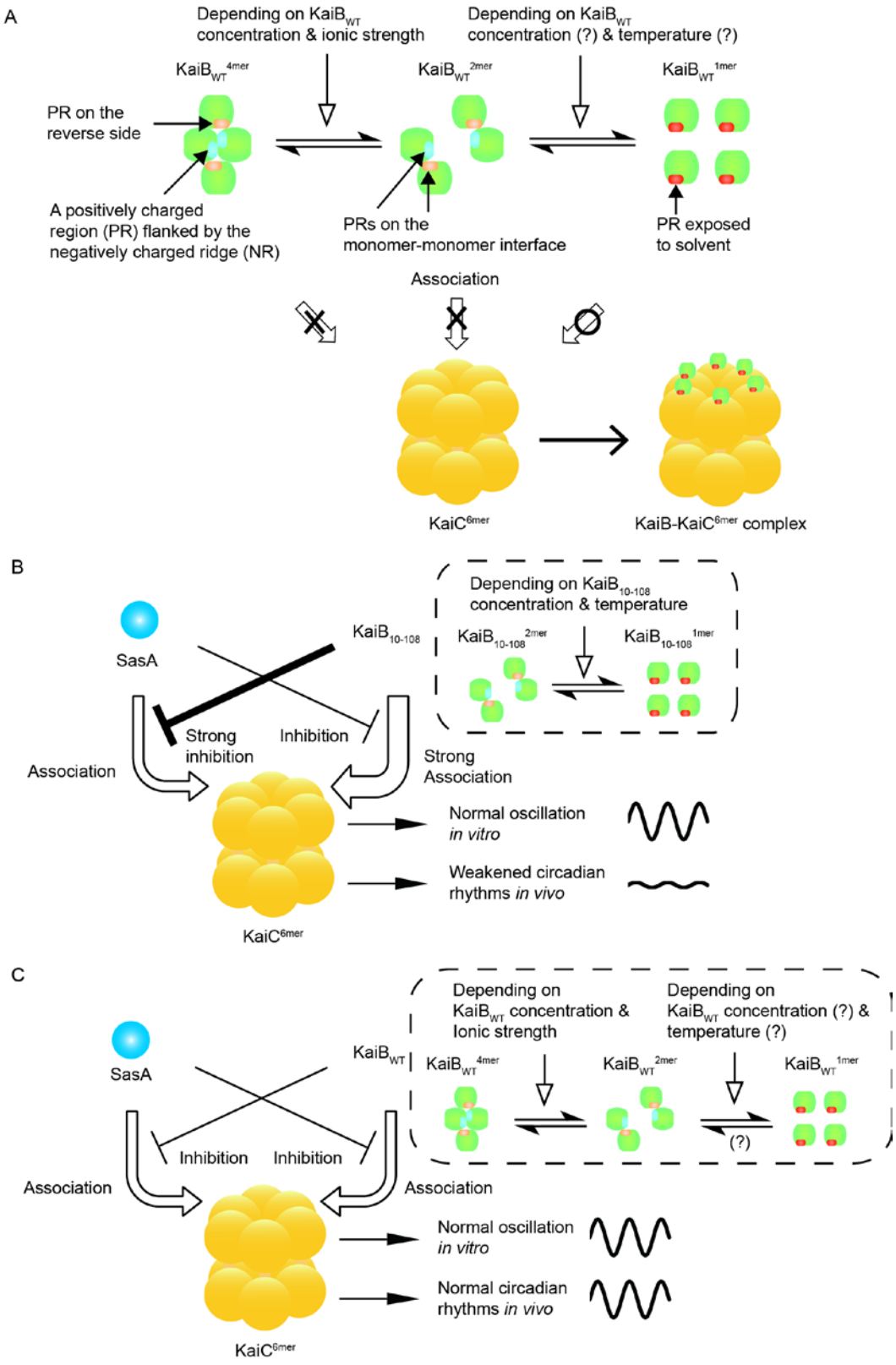
A
Depending on KaiB$_{WT}$ concentration & ionic strength
Depending on KaiB$_{WT}$ concentration (?) & temperature (?)
KaiB$_{WT}^{4mer}$
KaiB$_{WT}^{2mer}$
KaiB$_{WT}^{1mer}$
PR on the reverse side
A positively charged region (PR) flanked by the negatively charged ridge (NR)
PRs on the monomer-monomer interface
PR exposed to solvent
Association
KaiC^{6mer}
KaiB-KaiC^{6mer} complex
B
Depending on KaiB$_{10-108}$ concentration & temperature
KaiB$_{10-108}^{2mer}$
KaiB$_{10-108}^{1mer}$
SasA
KaiB$_{10-108}$
Strong inhibition
Inhibition
Association
Strong Association
Normal oscillation *in vitro*
Weakened circadian rhythms *in vivo*
KaiC^{6mer}
C
Depending on KaiB$_{WT}$ concentration & Ionic strength
Depending on KaiB$_{WT}$ concentration (?) & temperature (?)
KaiB$_{WT}^{4mer}$
KaiB$_{WT}^{2mer}$
KaiB$_{WT}^{1mer}$
(?)
SasA
KaiB$_{WT}$
Inhibition
Inhibition
Association
Association
Normal oscillation *in vitro*
Normal circadian rhythms *in vivo*
KaiC^{6mer}

Figure 9 A model for the oligomeric structure changes of KaiB, the association of KaiB with $KaiC^{6mer}$, and the regulation of KaiC-SasA complex formation by KaiB *via* its association with $KaiC^{6mer}$. (A) Oligomeric structure changes of KaiB and the association of KaiB with $KaiC^{6mer}$. $KaiB_{WT}$ exists in equilibrium between a monomer ($KaiB_{WT}{}^{1mer}$), dimer ($KaiB_{WT}{}^{2mer}$), and tetramer ($KaiB_{WT}{}^{4mer}$) depending on the KaiB concentration, ionic strength, and, most likely, temperature, although $KaiB_{WT}{}^{1mer}$ has not been detected. The PRs of $KaiB_{WT}$ are exposed to solvent upon dissociation of $KaiB_{WT}{}^{4mer}$ and $KaiB_{WT}{}^{2mer}$ into $KaiB_{WT}{}^{1mer}$. Six $KaiB^{1mer}$ molecules associate with one molecule of $KaiC^{6mer}$ (each N-terminal domain of the six subunits) *via* its PR, which is exposed to solvent at 40 °C. (B) Inhibition of KaiC-SasA complex formation by $KaiB_{10–108}$ *via* its strong association with $KaiC^{6mer}$. $KaiB_{10–108}$ exists in equilibrium between a monomer ($KaiB_{10–108}{}^{1mer}$) and dimer ($KaiB_{10–108}{}^{2mer}$) depending on the temperature and $KaiB_{10–108}$ concentration. SasA also associates with $KaiC^{6mer}$ *via* the KaiC N-terminal domain. Through its strong association with $KaiC^{6mer}$, $KaiB_{10–108}$ strongly inhibits KaiC-SasA complex formation, which is necessary for the generation of normal circadian gene expression rhythms in cyanobacterial cells. (C) Regulation of KaiC-SasA complex formation by KaiB *via* its association with $KaiC^{6mer}$. Through its proper association with $KaiC^{6mer}$, $KaiB_{WT}$ regulates the interaction of SasA with $KaiC^{6mer}$ and generates normal circadian gene expression rhythms in cyanobacterial cells. The tetramer form of KaiB is necessary for the generation of normal circadian gene expression rhythms in cells but not for the generation of circadian oscillations in the *in vitro* KaiABC clock oscillator.

Table 1 Molecular masses of KaiB proteins estimated with SE and GFC at various temperatures

KaiB	Temperature (°C)	Method	Molecular mass (kDa)	Oligomeric structure	*n*
$KaiB_{WT}$	4	SE	44.6	Tetramer	2
	35	SE	44.4 ± 1.8	Tetramer	3
$KaiB_{10–108}$	4	SE	12.8 ± 0.6	Monomer	3
	35	SE	28.4 ± 0.9	Dimer	3
$KaiB_{WT}$	4	GFC	66.7 ± 1.3^{+}	Tetramer^{+}	3
	40	GFC	65.1 ± 1.2^{+}	Tetramer^{+}	3
$KaiB_{1–94}$	4	GFC	24.8 ± 0.0	Dimer	3
	40	GFC	24.4 ± 0.8	Dimer	3
$KaiB_{10–108}$	4	GFC	23.5 ± 0.0^{+}	Monomer^{+}	3
	40	GFC	35.7 ± 0.0^{+}	Dimer^{+}	3

$KaiB_{10–108}$ and $KaiB_{WT}$ were incubated 4 °C or 35 °C for 16 h and then subjected to SE at 4 °C or 35 °C. $KaiB_{10–108}$, $KaiB_{WT}$, and $KaiB_{1–94}$ were incubated 4 °C or 40 °C for 6 h and then subjected to GFC at 4 °C. I calculated the molecular mass from the peak position of each elution profile. Other conditions were the same as described in the legend for Fig. 2F. Values are the mean ± S.D.

$^{+}$ $KaiB_{WT}{}^{4mer}$, $KaiB_{10\text{-}108}{}^{1mer}$, and $KaiB_{10\text{-}108}{}^{2mer}$ eluted as a single peak corresponding to a globular protein with molecular masses of 65-67 kDa, 23.5 kDa, and 35.7 kDa, respectively, in GFC.

Table 2 Molecular masses of KaiB proteins estimated with GFC at various KaiB concentrations

KaiB	KaiB concentration (μM)	Molecular mass (kDa)	Oligomeric structure
$KaiB_{WT}$	4.0	64.6 ± 0.0 (main peak)	Tetramer
		32.9 ± 0.6 (subpeak)	Dimer
	12	64.6 ± 0.0	Tetramer
	24	66.7 ± 1.3	Tetramer
	48	64.6 ± 0.0	Tetramer
$KaiB_{1–94}$	4.0	21.7 ± 0.4	Dimer
	12	23.7 ± 0.0	Dimer
	24	24.8 ± 0.0	Dimer
	48	25.4 ± 0.0	Dimer
$KaiB_{10–108}$	4.0	24.0 ± 0.4	Monomer
	12	24.0 ± 0.4	Monomer
	24	23.5 ± 0.0	Monomer
	48	23.8 ± 0.4	Monomer

$KaiB_{10–108}$, $KaiB_{WT}$, and $KaiB_{1–94}$ at the concentrations indicated were incubated at 4 °C for 6 h and then subjected to GFC at 4 °C. The two overlapping peaks for 4.0 μM $KaiB_{WT}$ were separated numerically using PeakFit (Systat, San Jose, CA, USA). I calculated the molecular mass from the peak position of each elution profile. Other conditions were the same as described in the legend for Fig. 2F. Values are the mean ± S.D. from triplicate measurements.

Table 3 Molecular mass of $KaiB_{WT}$ estimated with GFC at various NaCl concentrations and pH values

Buffer conditions	Molecular mass (kDa)	Oligomeric structure
20 mM MES-NaOH buffer (pH 5.5)		
containing 150 mM NaCl	63.4 ± 0.0	Tetramer
20 mM MES-NaOH buffer (pH 6.5)		
containing 150 mM NaCl	66.3 ± 1.3	Tetramer
20 mM Tris-HCl buffer (pH 8.5)		
containing 150 mM NaCl	65.6 ± 1.3	Tetramer
20 mM HEPES-NaOH buffer (pH 7.5)		
containing 150 mM NaCl	66.7 ± 1.3	Tetramer
300 mM NaCl	66.1 ± 1.3	Tetramer
500 mM NaCl	63.8 ± 1.3	Tetramer
1 M NaCl	63.6 ± 0.0 (main peak)	Tetramer
	36.8 ± 0.0 (subpeak)	Dimer

$KaiB_{WT}$ in the buffers indicated was incubated at 4 °C for 16 hours and then subjected to GFC in the buffers indicated at 4 °C. I calculated the molecular mass from the peak position of each elution profile. Other conditions were the same as described in the legend for Fig. 2F. Values for GFC are the mean ± S.D. from triplicate measurements.

Table 4 Kinetic and steady state parameters for the interaction of $KaiB_{WT}$, $KaiB_{1–94}$, and $KaiB_{10–108}$ with $KaiC_{DD}$ obtained with SPRanalysis

Protein	k_a	k_d	K_D
	$M^{-1}s^{-1}$ ($\times 10^6$)	s^{-1} ($\times 10^{-4}$)	M ($\times 0^{-9}$)
$KaiB_{WT}$	0.32 ± 0.17	9.4 ± 1.6	3.5 ± 1.5
$KaiB_{1–94}$	1.3 ± 0.30	5.9 ± 0.60	0.48 ± 0.14
$KaiB_{10–108}$	2.2 ± 0.029	4.0 ± 0.33	0.18 ± 0.017
"Preincubated $KaiB_{10–108}$"	0.84 ± 0.073	5.8 ± 0.55	0.70 ± 0.13

Values are the mean ± S.D. from triplicate measurements.

Table 5 Bioluminescence rhythms in P_{psbA1}::*Xl luxAB* reporter strains of *T. elongatus* expressing $KaiB_{WT}$ or KaiB mutants

Strain	Period (h)	Phase (h)	Amplitude	*n*
WT	24.6 ± 0.2	2.9 ± 0.4	1.27 ± 0.03	7
$KaiB_{null}$	-	-	-	8
$KaiB_{WT}$	25.3 ± 0.6	1.3 ± 0.4	1.29 ± 0.04	7
$KaiB_{1–94}$	26.4 ± 1.6	3.2 ± 1.9	1.07 ± 0.06	10
$KaiB_{10–108}$ (rhythmic)	24.0	11.1	1.03	2

Among the 12 samples expressing $KaiB_{10–108}$, ten samples showed arrhythmic bioluminescence, and only two samples showed bioluminescence rhythms. Values were calculated from the results shown in Fig. 7B.

References

(1) Murakami, R., Mutoh, R., Iwase, R., Furukawa, Y., Imada, K., Onai, K., Morishita, M., Yasui, S., Ishii, K., Valencia, J.S., Uzumaki, T., Namba, K. & Ishiura, M. (2012) The roles of the dimeric and tetrameric structures of the clock protein KaiB in the generation of circadian oscillations in cyanobacteria. *J. Biol. Chem.* **287**, 29506-29515.

(2) Bünning, E. (1973) The physiological clock: circadian rhythms and biological chronometry, 3rd ed. New York, N. Y.: Springer-Verlag.

(3) Kondo, T. & Ishiura, M. (1999) The circadian clocks of plants and cyanobacteria. *Trends Plant Sci.* **4**, 171-176.

(4) Grobbelaar, N., Huang, T.C., Lin, H.Y. & Chow, T.J. (1986) Dinitrogen-fixing endogenous rhythm in *Synechococcus* RF-1. *FEMS Microbiol. Lett.* **37**, 173-177.

(5) Ishiura, M., Kutsuna, S., Aoki, S., Iwasaki, H., Andersson, C.R., Tanabe, A., Golden, S.S., Johnson, C.H. & Kondo, T. (1998) Expression of a gene cluster *kaiABC* as a circadian feedback process in cyanobacteria. *Science* **281**, 1519-1523.

(6) Iwasaki, H., Williams, S.B., Kitayama, Y., Ishiura, M., Golden, S.S. & Kondo, T. (2000) A kaiC-interacting sensory histidine kinase, SasA, necessary to sustain robust circadian oscillation in cyanobacteria. *Cell* **101**, 223-233.

(7) Takai, N., Nakajima, M., Oyama, T., Kito, R., Sugita, C., Sugita, M., Kondo, T. & Iwasaki, H. (2006) A KaiC-associating SasA-RpaA two-component regulatory system as a major

circadian timing mediator in cyanobacteria. *Proc. Natl. Acad. Sci. USA* **103**, 12109-12114.

(8) Taniguchi, Y., Katayama, M., Ito, R., Takai, N., Kondo, T. & Oyama, T. (2007) *labA*: a novel gene required for negative feedback regulation of the cyanobacterial circadian clock protein KaiC. *Genes Dev.* **21**, 60–70.

(9) Schmitz, O., Katayama, M. Williams, S.B., Kondo, T., Golden, S.S. (2000) CikA, a bacteriophytochrome that resets the cyanobacterial circadian clock. *Science* **289**, 765-768.

(10) Kutsuna, S., Kondo, T., Aoki, S., & Ishiura, M. (1998) A period-extender gene, *pex*, that extends the period of the circadian clock in the cyanobacterium *Synechococcus* sp. strain PCC 7942. *J. Bacteriol*. **180**, 2167-2174.

(11) Takai, N., Ikeuchi, S., Manabe, K., & Kutsuna, S. (2006) Expression of the circadian clock-related gene pex in cyanobacteria increases in darkness and is required to delay the clock. *J. Biol. Rhyth.* **21**, 235-244.

(12) Nakajima, M., Imai, K., Ito, H., Nishiwaki, T., Murayama, Y., Iwasaki, H., Oyama, T. & Kondo, T. (2005) Reconstitution of circadian oscillation of cyanobacterial KaiC phosphorylation *in vitro*. *Science* **308**, 414-415.

(13) Terauchi, K., Kitayama, Y., Nishiwaki, T., Miwa, K., Murayama, Y., Oyama, T. & Kondo, T. (2007) ATPase activity of KaiC determines the basic timing for circadian clock of cyanobacteria. *Proc. Natl. Acad. Sci. USA* **104**, 16377-16381.

(14) Kageyama, H., Nishiwaki, T., Nakajima, M., Iwasaki, H., Oyama, T. & Kondo, T. (2006)

Cyanobacterial circadian pacemaker: Kai protein complex dynamics in the KaiC phosphorylation cycle *in vitro*. *Mol. Cell* **23**, 161-71.

(15) Akiyama, S., Nohara, A., Ito, K. & Maéda, Y. (2008) Assembly and disassembly dynamics of the cyanobacterial periodosome. *Mol. Cell* **29**, 703-716.

(16) Garces, R.G., Wu, N., Gillon, W. & Pai, E.F. (2004) Anabaena circadian clock proteins KaiA and KaiB reveal a potential common binding site to their partner KaiC. *EMBO J.* **23**, 1688-1698.

(17) Uzumaki, T., Fujita, M., Nakatsu, T., Hayashi, F., Shibata, H., Itoh, N., Kato, H. & Ishiura, M. (2004) Crystal structure of the C-terminal clock-oscillator domain of the cyanobacterial KaiA protein. *Nat. Struct. Mol. Biol.* **11**, 623-631.

(18) Ye, S., Vakonakis, I., Ioerger, T.R., LiWang, A.C. & Sacchettini, J.C. (2004) Crystal structure of circadian clock protein KaiA from *Synechococcus elongatus*. *J. Biol. Chem.* **279**, 20511-20518.

(19) Hayashi, F., Iwase, R., Uzumaki, T. & Ishiura, M. (2006) Hexamerization by the N-terminal domain and intersubunit phosphorylation by the C-terminal domain of cyanobacterial circadian clock protein KaiC. *Biochem. Biophys. Res. Commun.* **348**, 864-872.

(20) Murakami, R., Miyake, A., Iwase, R., Hayashi, F., Uzumaki, T., Ishiura, M. (2008) ATPase activity and its temperature compensation of the cyanobacterial clock protein KaiC. *Genes Cells* **13**, 387-95.

(21) Iwasaki, H., Nishiwaki, T., Kitayama, Y., Nakajima, M. & Kondo, T. (2002) KaiA-stimulated KaiC phosphorylation in circadian timing loops in cyanobacteria. *Proc. Natl. Acad. Sci. USA* **99**, 15788-15793.

(22) Williams, S.B., Vakonakis, I., Golden, S.S. & LiWang, A.C. (2002) Structure and function from the circadian clock protein KaiA of *Synechococcus elongatus*: A potential clock input mechanism. *Proc Natl Acad Sci USA* **99**, 15357-15362.

(23) Hayashi, F., Ito, H., Fujita, M., Iwase, R., Uzumaki, T. & Ishiura, M. (2004) Stoichiometric interactions between cyanobacterial clock proteins KaiA and KaiC. *Biochem. Biophys. Res. Commun.* **316**, 195-202.

(24) Mutoh, R., Mino, H., Murakami, R., Uzumaki, T., Takabayashi, A., Ishii, K. & Ishiura, M. (2010) Direct interaction between KaiA and KaiB revealed by a site-directed spin labeling electron spin resonance analysis. *Genes Cells* **15**, 269-280.

(25) Xu, Y., Mori, T. & Johnson, C.H. (2003) Cyanobacterial circadian clockwork: roles of KaiA, KaiB and the *kaiBC* promoter in regulating KaiC. *EMBO J.* **22**, 2117-2126.

(26) Egli, M., Mori, T., Pattanayek, R., Xu, Y., Qin, X. & Johnson, C.H. (2012) Dephosphorylation of the core clock protein KaiC in the cyanobacterial KaiABC circadian oscillator proceeds *via* an ATP synthase mechanism. *Biochem.* **51**, 1547-1558.

(27) Nishiwaki, T., Kondo, T. (2012) Circadian autodephosphorylation of cyanobacterial clock protein KaiC occurs *via* formation of ATP as intermediate. *J. Biol. Chem.* **287**, 18030-18035.

(28) Mori, T., Saveliev, S.V., Xu, Y., Stafford, W.F., Cox, M.M., Inman, R.B., Johnson, C.H. (2002) Circadian clock protein KaiC forms ATP-dependent hexameric rings and binds DNA. *Proc. Natl. Acad. Sci. USA.* **99**, 17203-17208.

(29) Hayashi, F., Suzuki, H., Iwase, R., Uzumaki, T., Miyake, A., Shen, J.R., Imada, K., Furukawa, Y., Yonekura, K., Namba, K. & Ishiura, M. (2003) ATP-induced hexameric ring structure of the cyanobacterial circadian clock protein KaiC. *Genes Cells* **8**, 287-296.

(30) Pattanayek, R., Wang, J., Mori, T., Xu, Y., Johnson, C.H. & Egli, M. (2004) Visualizing a circadian clock protein: crystal structure of KaiC and functional insights. *Mol. Cell* **15**, 375-388.

(31) Hitomi, K., Oyama, T., Han, S.G., Arvai, A.S. & Getzoff, E.D. (2005) Tetrameric architecture of the circadian clock protein KaiB - a novel interface for intermolecular interactions and its impact on the circadian rhythm. *J. Biol. Chem.* **280**, 19127-19135.

(32) Iwase, R., Imada, K., Hayashi, F., Uzumaki, T., Morishita, M., Onai, K., Furukawa, Y., Namba, K. & Ishiura, M. (2005) Unique homo-tetrameric structure and functionally important sub-structures of the circadian clock protein KaiB. *J. Biol. Chem.* **280**, 43141-43149.

(33) Pattanayek, R., Williams, D.R., Pattanayek, S., Mori, T., Johnson, C.H., Stewart, P.L. & Egli, M. (2008) Structural model of the circadian clock KaiB-KaiC complex and mechanism for modulation of KaiC phosphorylation. *EMBO J.* **27**, 1767-1778.

(34) Mutoh, R., Nishimura, A., Yasui, S., Onai, K. & Ishiura, M. (2013) The ATP-mediated regulation of KaiB-KaiC interaction in the cyanobacterial circadian clock. *PLoS ONE* **8**, e80200.

(35) Kitayama, Y., Iwasaki, H., Nishiwaki, T. & Kondo, T. (2003) KaiB functions as an attenuator of KaiC phosphorylation in the cyanobacterial circadian clock system. *EMBO J.* **22**, 2127-2134.

(36) Valencia, S.J., Bitou, K., Ishii, K., Murakami, R., Morishita, M., Onai, K., Furukawa, Y., Imada, K., Namba, K. & Ishiura, M. (2012) Phase-dependent generation and transmission of time information by the KaiABC circadian clock oscillator through SasA-KaiC interaction in cyanobacteria. *Genes Cells* **17**, 398-419.

(37) Taniguchi, Y., Takai, N., Katayama, M., Kondo, T. & Oyama, T. (2010) Three major output pathways from the KaiABC-based oscillator cooperate to generate robust circadian *kaiBC* expression in cyanobacteria. *Proc. Natl. Acad. Sci. USA* **107**, 3263-3268.

(38) Takai, N., Ikeuchi, S., Manabe, K., and Kutsuna, S. (2006) Expression of the circadian-clock-related gene *pex* in cyanobacteria increases in darkness and is required to delay the clock. *J. Biol. Rhythms*. **4**, 235-44.

(39) Arita, K., Hashimoto, H., Igari, K., Akaboshi, M., Kutsuna, S., Sato, M., & Shimizu, T. (2007) Structural and biochemical characterization of a cyanobacterium circadian clock-modifier protein. *J. Biol. Chem.* **282**, 1128-35.

(40) Kurosawa, S., Murakami, R., Onai, K., Morishita, M., Hasegawa, D., Iwase, R., Uzumaki, T., Hayashi, F., Kitajima-Ihara, T., Sakata, S., Murakami, M., Kouyama, T. & Ishiura, M. (2009) Functionally important structural elements of the cyanobacterial clock-related protein Pex. *Genes Cells* **14**, 1-16.

(41) Kutsuna, S., Kondo, T., Ikegami, H., Uzumaki, T., Katayama, M. & Ishiura, M. (2007) The circadian clock-related gene *pex* regulates a negative cis element in the *kaiA* promoter region. *J. Bacteriol.* **189**, 7690-7696.

(42) Yamaoka, T., Satoh, K., & Katoh, S. (1978) Photosynthetic activities of a thermophilic blue-green alga. *Plant Cell Physiol.* **19**, 943-954.

(43) Bradford, M. M., (1976) A rapid and sensitive method for the quantitation of microgram quantities of protein utilizing the principle of protein-dye binding. *Anal. Biochem.* **72**, 248-254.

(44) Laue, T. M., Shah, B. D., Ridgeway, T. M. & Pelletier S. L. (1992) Computer-aided interpretation of analytical sedimentation data for proteins. In: *Analytical ultracentrifugation in biochemistry and polymer science* (eds S. E. Harding, A. J. Rowe & J. C. Horton), pp. 90-125. Cambridge, Cambridgeshire: Royal Society of Chemistry.

(45) Laemmli, U.K. (1970) Cleavage of structural proteins during the assembly of the head of bacteriophage T4. *Nature* **227**, 680-685.

(46) Smith, P.K., Krohn, R.I., Hermanson, G.T., Mallia, A.K., Gartner, F.H., Provenzano, M.D.,

Fujimoto, E.K., Goeke, N.M., Olson, B.J. & Klenk, D.C. (1985) Measurement of protein using bicinchoninic acid. *Anal. Biochem*. **150**, 76–85.

(47) Okamoto, K., Onai, K. & Ishiura, M. (2005) RAP, an integrated program for monitoring bioluminescence and analyzing circadian rhythms in real time. *Anal. Biochem.* **340**, 193-200.

(48) Onai, K., Morishita, M., Itoh, S., Okamoto, K. & Ishiura, M. (2004) Circadian rhythms in the thermophilic cyanobacterium *Thermosynechococcus elongatus*: compensation of period length over a wide temperature range. *J. Bacteriol.* **186**, 4972-4977.

(49) Nelson, W., Tong, Y.L., Lee, J.K. & Halberg, F. (1979) Methods for cosinor-rhythmometry. *Chronobiol*. **6**, 305-323.

(50) Laue, T. M. & Rhodes D. G. (1990) Determination of size, molecular weight, and presence of subunits. In: *Methods in Enzymology* (ed M. P. Deutscher), **182**, 566-587. San Diego, California: Academic Press.

(51) Villarreal, S.A., Pattanayek, R., Williams, D.R., Mori, T., Qin, X., Johnson, C.H., Egli, M. & Stewart, P.L. (2013) CryoEM and molecular dynamics of the circadian KaiB-KaiC complex indicates that KaiB monomers interact with KaiC and block ATP binding clefts. *J. Mol. Biol.* **425**, :3311-24.

Acknowledgments

I appreciate Professor Emeritus Masahiro Ishiura for helpful discussion and advice. I also appreciate Research Associate Risa Mutoh of Osaka University for helpful advice and discussions and Professor Keiichi Namba and Project Researcher Yukio Furukawa of Osaka University for technical support. I thank Dr. Kiyoshi Onai, Megumi Morishita, Satoko Ogawa and Kumiko Tanaka for technical support. I also thank all members in Ishiura's laboratory for kind support. As a research assistant, I was supported by a Global Center of Excellence grant from MEXT.